JOURNAL

OF THE

IMPERIAL FISHERIES INSTITUTE

Vol. XXX, No. 4. March, 1935.

Circulation of Air in a Cold-Storage Warehouse. II. Reproduction in Models of the Observed Original Circulations.

(Pls. XXXII, XXXIII)

By Mituyo OKADA.

(Received March 20, 1935)

Introduction.

In the preliminary study with the two-dimensional fundamental circulations of air produced by natural convection in a rectangular chamber cooled above and heated below, the author[1] has deduced a pair of laws which give the relation of original convections of air on a large scale to the ones reproduced in models. The laws were derived by the aid of the principle of dynamical similarity from BOUSSINESQ[2] and Lord RAYLEIGH's[3] hydrodynamical and thermometric equations of natural convection in the steady state, under the assumption, that the velocity and linear dimension of the haphazard eddies accompanied by the general motion of air vary as the velocity and as the linear dimension, respectively, of the general circulations. They are :—

1. Whenever the distribution of temperature on the similar boundaries is similar, the distribution of temperature at any point as well as the velocity of the general flow becomes similar in the steady state.

(1) OKADA, M.: Circulation of air in a cold-storage warehouse. I. Preliminary experiments on convection current in a rectangular chamber cooled above and heated below. J. Imper. Fisher. Inst., **26** (2), 1931, 69–78.

(2) BOUSSINESQ, J.: Théorie analytique de la chaleur. **2**, Paris 1903, 174.

(3) Lord RAYLEIGH: On the convection current in a horizontal layer of fluid, when the higher temperature is on the upper side. Phil. Mag., **32**, 1916, 529.

2. The relation between the velocity, V, and the linear dimension, L, of the general circulation and the local temperature difference, $\Delta\theta$, is given by $V \propto (L.\Delta\theta)^{\frac{1}{2}}$.

It was shown that the laws were satisfied by the results of the preliminary experiments stated above. In order to ascertain whether or not they can be utilized really in the comparison of the circulations in models with their originals, several observations were undertaken in a cold-storage warehouse in operation and their reproduction in models was tried in laboratory experiments.

Observation of the original circulations.

In the summer of 1930, the Tobata Cold-Stroage Company generously put the cold-storage warehouse belonging to the company at the author's disposal for the observation in several parts of it. In some of chambers of the warehouse, there were frozen fishes in storage in wooden boxes, piled in rectangular blocks, leaving the spaces of the shape of nearly rectangular narrow passages, while in one of the chambers, the air-freezing of a number of fishes, *Nibea manchurica* (J. & T.), was going on in the back half of the chamber and the space remaining in the other half was widely stretched in three dimensions. The circulations of air in both kinds of such spaces were studied.

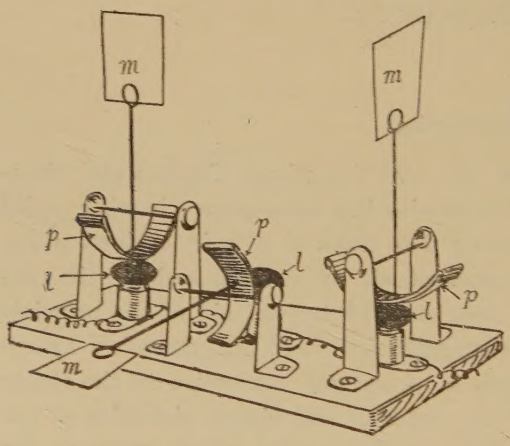

Fig. 1 A set of the current meter. m: mica plate, p: photographic sensitive paper, l: enameled electric lamp with a pin-hole.

For the observation of very weak velocity of the general circulation, a kind of optically registering current meter was devised, which is composed of a set of three pendulums, each intended to give each of the three perpendicular components of the velocity(1).

(1) A brief preliminary account on the current meter with some of the results obtained both in the original case and in the models was made by the author. OKADA, M.: Steady circulation of air in a cold-storage warehouse produced by natural convection and its reproduction in models Bull. of the Jap. Soc. Sci. Fisher., 1 (4), 1932, 171–177, in Japanese with English resumé.

A pendulum is made of iron wire, 0.7 mm. in diameter, and about 7 cm. in length, bent at its one end in small double loops, to which a piece of thin trapezoidal mica plate, about 10 cm.^{2} in area, is inserted, the axis of symmetry of the plate being on the extension line of the straight part of the wire. At the other end of the wire a piece of an elongated rectangular zinc plate, about 0.9 cm. wide and about 5 cm. long, is soldered at right angles at its center. The zinc plate is bent in a form of semicircular arc of radius of about 2 cm., the wire being on the concave side of the arc. The plate has the orientation such that its longer curved sides lie in perpendicular planes to the mica plate. Both ends of the zinc plate are folded back to the convex side to form each a groove. In operation, a rectangular piece of photographic sensitive paper is supported at its both ends by these grooves so as to fit on the convex surface of the zinc plate, and the pendulum is thus balanced about the supporting pins, soldered at right angles to the wire in coincidence with the axis of the cylindrical surface of the zinc plate. With the ends of the pins, just mentioned, the pendulum is mounted on a pair of pillars, made of zinc plates, which are fixed on a wooden pedestal of the current meter. By adjusting the balance, the neutral orientation of the pendulum is to be made horizontal or vertical. Three pendulums are so arranged that the mica plates, when balanced and acted by no wind, face each perpendicular to each. On the pedestal, besides three pairs of pillars, three tiny electric lamps are fixed so as to face each to the centre of the zinc plate of each pendulum. Each lamp is enameled, leaving a pin-hole against the photographic paper on the zinc plate, and the light from the filament casts a spot on the photographic paper through the pin-hole.

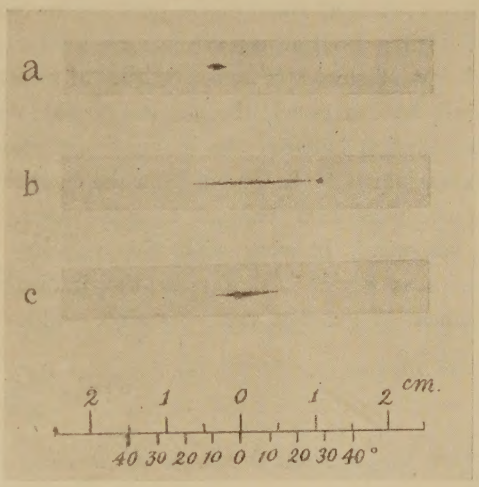

Fig. 2 An example showing the records of the current meter.

In the observation, several sets of current meters were put each on a wooden board, hanging with ropes at the desired place in the space. Each current meter was first covered with a pasteboard box so that no wind should

act on it, and the lamp was lighted for several minutes, then the box was removed and the current meter was exposed to the circulating air, the lamp having been lighted by itself for about half an hour. By developing the sensitive paper, we obtain the records of inclination of the pendulum due to the action of wind with a spot indicating the zero-point. An example of a set of such records is shown in Fig. 2.

The constant of the current meter was determined by the following calibration, for which, however, we could have no good wind channel at Tobata, except a small pasteboard box, about 50 cm. long, 30 cm. high and 25 cm. broad, without both the end sides. The box was placed in the wind blowing at some parts of an auxilliary building of the warehouse, or in the wind got from an electric fan. The pendulums were put one by one on the pillars fixed at the middle part of the channel and the inclination was read off with a graduating circle, while the speed of the wind, visualized with patches of smoke of senkô, a kind of incense, was measured with a stop-watch. As it was expected, the results of the calibration was not very accurate, so the relation between the inclination of the pendulum and the velocity of wind was assumed to be given from the condition that the moments of forces acting on the pendulum balance to each other. The moment of the resistance due to the wind, blowing with the velocity v perpendicular to the mica plate varies as $v^2\cos^2\theta$[1], so far as the inclination θ is not very great, while the moment of gravity varies as $\sin\theta$. Thus we have

$$v^2 = k\frac{\sin\theta}{\cos^2\theta},$$

where the constant k can be determined from the results of the calibration. In the present case, k was determined graphically. The measurement of the temperature was made with U-shaped toluene-mercury maximum, and minimum thermometers. They were placed at the desired positions while the observation of the velocity was going on. As the entrance of observers into the chamber would heat the air in it, the minimum temperatures were read off as the representative of the temperatures. The readings of the thermometers were calibrated in the chamber, by placing the thermometers all together with a standardized mercury thermometer in a box, and the correction was

(1) That the force acted by the wind on the semicircular arc of the zinc plate has little moment about the central line is shown experimentally, as it is expected from the theory given, for example, by W. G. BIRKLEY: Some two-dimensional potential problems connected with the circular arc. Phil. Mag., **35**, 1918, 396; **36**, 1918, 273.

carried out to 0.1°C. In some cases the correction exceeded 1°C in its absolute value.

Discussions on the records obtained with the current meter.

When the current meter is placed in the circulating air, and the pendulums are inclined, the horizontal pendulum, for example, is not only acted by the vertical flow of air but also by the horizontal component of the flow. But the moment of force due to the latter varies nearly as $\sin^2\theta$, so it was assumed that this effect was negligible.

The records of inclination obtained show that the wind was accompanied by fluctuations due to the turbulence. In some cases, where the fluctuations were great, it was difficult to determine at once the mean inclination from the records, which delineated a long line, as shown in Fig. 2, b. In such a case, we took the mean of the two terminal inclinations at which the blackness of the record was recognized as to be equal. The error in the mean velocity introduced by such approximation can be estimated as follows:—

It is generally ascertained[1] with the atmospheric winds that the distribution of the fluctuations in velocity due to the turbulence obeys Maxwell's law such as

$$f(v-v_0)=\frac{1}{\sqrt{2\pi}\sigma}e^{-\frac{(v-v_0)^2}{2\sigma^2}},$$

where v is a component of the velocity, v_0 that of the general flow, or the mean value of v, and $f(v-v_0)\,dv$ is the frequency of the said component lying in the range $v\sim v+dv$. Assuming that the same is the case with the present circulations, we can calculate, as follows, the frequency, $F(\theta)\,d\theta$, of the inclination of pendulum lying in the range $\theta\sim\theta+d\theta$. Since $v=\frac{\sqrt{k}\sin^{\frac{1}{2}}\theta}{\cos\theta}$, $\frac{dv}{d\theta}$ $=\frac{\sqrt{k}}{2}\frac{1+\sin\theta}{\sin^{\frac{1}{2}}\theta\cos^2\theta}\fallingdotseq\frac{\sqrt{k}}{2}\frac{1+\frac{19}{12}\theta^2}{\sqrt{\theta}}$; and $v-v_0=(\theta-\theta_0)\left(\frac{dv}{d\theta}\right)_0$[2], where θ_0 corresponds to the mean velocity. Hence,

$$F(\theta)=\frac{\sqrt{k}}{2\sqrt{2\pi}\sigma}e^{-\frac{(\theta-\theta_0)^2}{2\sigma^2\left(\frac{d\theta}{dv}\right)_0^2}}\frac{1+\frac{19}{12}\theta^2}{\sqrt{\theta}}.$$

(1) For example, see FUJIWHARA, S.: On the structure of wind and Robinson constant. Geophys. Mag., **6** (1), 1932, 19–32. Part I, Structure of wind.

(2) Since $\frac{dv}{d\theta}=\infty$ at $\theta=0$, we must consider the case, where $\theta\theta_0>0$.

Thus $F(\theta)$ becomes ∞ at $\theta=0$. For the brevity's sake, let us consider the case where $\theta>0$. We can say that, when the blackness of the record at $\theta=\theta_1$ and $\theta=\theta_2$ $(\theta_1>\theta_2)$ is equal, $F(\theta_1)=F(\theta_2)$. Thus we have

$$e^{-\frac{(\theta_2-\theta_0)^2}{2\sigma^2\left(\frac{d\theta}{dv}\right)_0^2}}\frac{1+\frac{19}{12}\theta_2^\circ}{\sqrt{\theta_2}}=e^{-\frac{(\theta_1-\theta_0)^2}{2\sigma^2\left(\frac{d\theta}{dv}\right)_0^2}}\frac{1+\frac{19}{12}\theta_1^\circ}{\sqrt{\theta_1}},$$

from which we get

$$\frac{(\theta_1-\theta_0)^2-(\theta_2-\theta_0)^2}{2\sigma^2\left(\frac{d\theta}{dv}\right)_0^2}=\log\left(\frac{1+\frac{19}{12}\theta_1^\circ}{1+\frac{19}{12}\theta_2^\circ}\sqrt{\frac{\theta_2}{\theta_1}}\right),$$

$$\therefore\quad\frac{(\theta_1-\theta_2)(\theta_1+\theta_2-2\theta_0)}{2\sigma^2\left(\frac{d\theta}{dv}\right)_0^2}\fallingdotseq\frac{19}{12}(\theta_1^\circ-\theta_2^\circ)-\frac{1}{2}\frac{\theta_1-\theta_2}{\theta_1},$$

or

$$\frac{\theta_1+\theta_2}{2}-\theta_0=\frac{\sigma^2\left(\frac{d\theta}{dv}\right)_0^2}{\theta_1-\theta_2}\left\{\frac{19}{12}(\theta_1^\circ-\theta_2^\circ)-\frac{1}{2}\frac{\theta_1-\theta_2}{\theta_1}\right\}.$$

It can be assumed that generally $\sigma\left(\frac{d\theta}{dv}\right)_0<\frac{\theta_1-\theta_2}{2}$, and then

$$\left|\frac{\theta_1+\theta_2}{2}-\theta_0\right|<\left|\frac{\theta_1-\theta_2}{4}\left\{\frac{19}{12}(\theta_1^\circ-\theta_2^\circ)-\frac{1}{2}\frac{\theta_1-\theta_2}{\theta_1}\right\}\right|.$$

The values of the term on the right hand side are, as given in Table I, mostly small.

Table I.

θ_1	θ_2	$\frac{\theta_1-\theta_2}{4}\left\{\frac{19}{12}(\theta_1^\circ-\theta_2^\circ)-\frac{1}{2}\frac{\theta_1-\theta_2}{\theta_1}\right\}$
0.8	0.6	0.02
„	0.4	0.05
„	0.2	0.09
0.6	0.4	0.01
„	0.2	0.02
0.4	0.2	−0.003

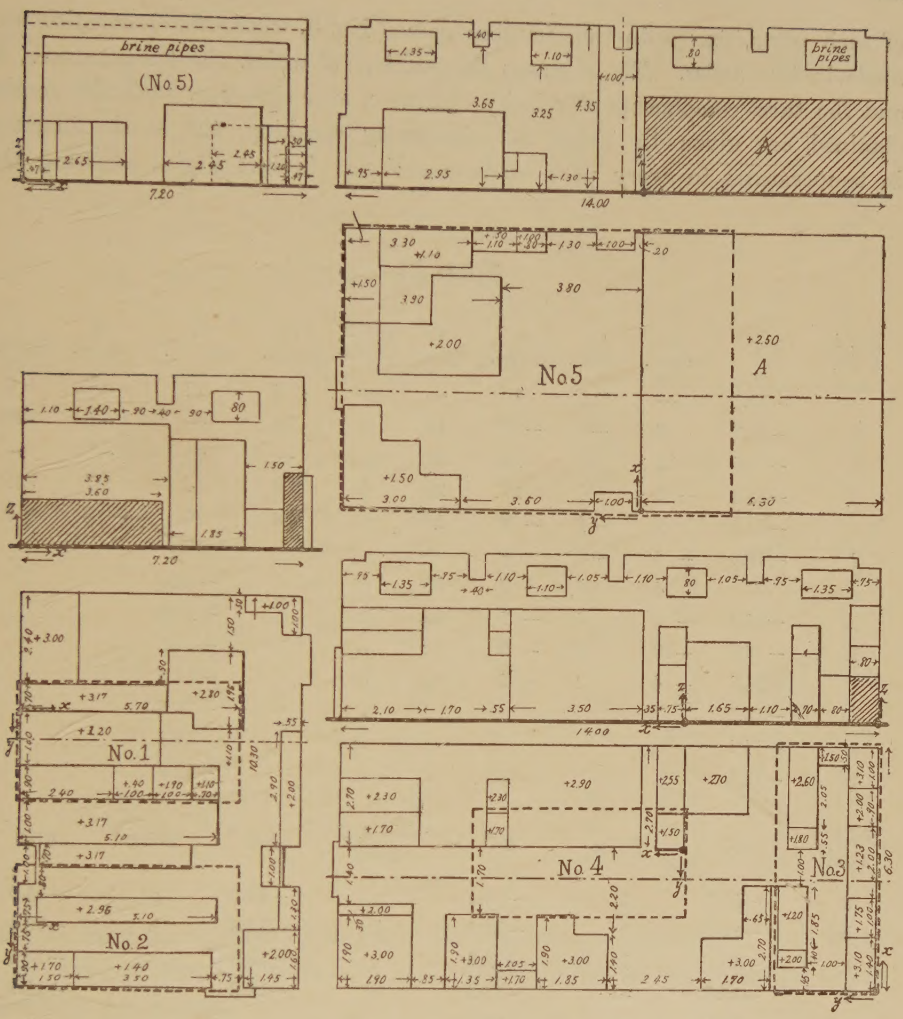

Fig. 3 The arrangement of wares in several chambers of the cold-storage warehouse. Thick broken lines show the parts of which the models were prepared in the experiments. A: The block of fishes under air-freezing. Lengths and heights are given in meters.

The original circulations observed.

The arrangement of the wares in the chambers observed was as shown in Fig. 3. The thick broken lines show the parts, of which the models were constructed afterwards in the laboratory experiments. The observation of the temperatures and velocities was made simultaneously at various points in each

of such parts, except in the chamber named No. 5, where the observation was made in two series. Fig. 4 shows the positions at which the temperatures, θ, and the three components of velocity of flow, v, were observed, while the results obtained are given in Table II. Generally speaking, the local difference in temperatures in every part above mentioned is but slight, showing the

Table II

No. 1 Point	θ°C	v_x cm/sec.	v_y cm/sec.	v_z cm/sec.	v cm/sec.
a	−13.1	—	8	10	—
b	−13.7	3	−9	− 9	10
c	−13.6	11	0	28	30
d	−13.8	− 6	0	27	28
e	−13.4	9	−4	− 9	13
f	−13.9	− 6	−3	—	—
g	—	4	6	− 9	10
h	−13.2	− 9	6	− 7	11
k	−13.3	−10	3	− 5	11
l	−13.6	− 4	3	−12	13
m	−13.7				
n	−14.1				
p	−13.5				

No. 2 Point	v_x cm/sec.	v_y cm/sec.	v_z cm/sec.	v cm/sec.
a	6	15	−7	9
b	13	—	−8	16
c	—	—	−7	—
d	9	4	7	11
e	4	0	8	9

	θ°C
f	−12.0
g	−12.2
h	−12.2
k	−11.8
l	−12.2
m	−12.4
n	−12.0

No. 3, 1 Point	θ°C	Point	θ°C
a	−13.6	h	−13.4
b	−13.6	k	−13.6
c	−13.6	l	−12.5
d	−13.6	m	−13.2
e	−13.8	n	−13.3
f	−13.5	p	−13.6
g	−13.5		

	v_x cm/sec.	v_y cm/sec.	v_z cm/sec.	v cm/sec.
e	5	—	9	10
l	−18	15	10	21
m	—	10	− 6	—
n	12	—	—	—
r	−12	−6	− 7	14

No. 3, 2 Point	θ°C	Point	θ°C
a	−13.7	g	−13.0
b	−14.3	h	−13.0
c	−13.3	k	−13.3
d	−13.2	l	−12.9

	v_x cm/sec.	v_y cm/sec.	v_z cm/sec.	v cm/sec.
e	6	5	− 7	9
f	6	− 6	0	6
g	−8	10	7	10
h	−8	−10	6	10

No. 4 Point	θ°C	v_x cm/sec.	x_y cm/sec.	v_z cm/sec.	v cm/sec.	Point	θ°C	v_x cm/sec.	v_y cm/sec.	v_z cm/sec.	v cm/sec.
a	−13.3	—	—	—	—	g	−14.2	—	—	—	—
b	−15.4	9	−13	−6	11	h	−13.6	−5	5	5	6
c	−13.1					k	−14.3	−3	−14	9	9
c′		3	− 7	8	9	l	−13.8	10	− 4	16	19
d	−13.9	−8	0	23	24	m	−13.9	9	− 5	5	11
e	−14.0					n	−13.7	—	—	4	—
f	−14.0	−5	− 5	−5	7						

No. 5 Point	θ°C	v_x cm/sec.	v_y cm/sec.	v_z cm/sec.	Point	θ°C	x_x cm/sec.	v_y cm/sec.	v_z cm/sec.
a	−7.2				k	−8.3			
b	−7.7				l	−8.3			
c	−7.2				m	−7.9			
d	−7.5	7.3	−3.4	− 6.5	n	−7.7			
d′		5.2	—	5.0	o	−8.0	7.5	− 6.5	−11.5
e	−8.0				p		4.4	− 5.4	− 2.6
e′		16.6	5.8	25.0	q′		9.2	− 3.6	−12.0
f′		6.2	−1.8	10.1	q	−8.4			
f	−7.6				q″		−11.0	− 4.4	17.3
g′		−5.6	7.2	8.7	r		4.0	0.0	9.7
g	−7.6	−7.4	5.5	6.7	s	−7.9	−13.3	2.3	−10.2
h	−7.8	18.0	6.4	22.2	t	−8.1	23.6	−11.6	16.4
i	−8.5	18.2	10.3	3.4	u	−8.1	32.6	13.0	25.8
j	−7.7	12.8	−11.0	16.0	v	−7.9	9.8	6.4	13.2
					w	−7.9	26.2	−10.2	4.7

excellent function of those chambers of the cold-storage warehouse. The speed of the general circulations is also very small, being of the order of a few decimeters per second.

In the chamber No. 5 there was going on the air-freezing of fishes as mentioned already. In the remaining space of the chamber, there were several blocks of frozen fishes in wooden boxes. Some of them were brought there from the other far colder chambers just before the observation was commenced. Strictly speaking, therefore, the circulation of air in it could not be in steady state. The temperature of the colder wares was not measured, owing to the lack of thermometers, but it was estimated to range from −10°C to −13°C. It is evident, however, from the results obtained, that the circulation of air in it was mainly maintained by the natural convection

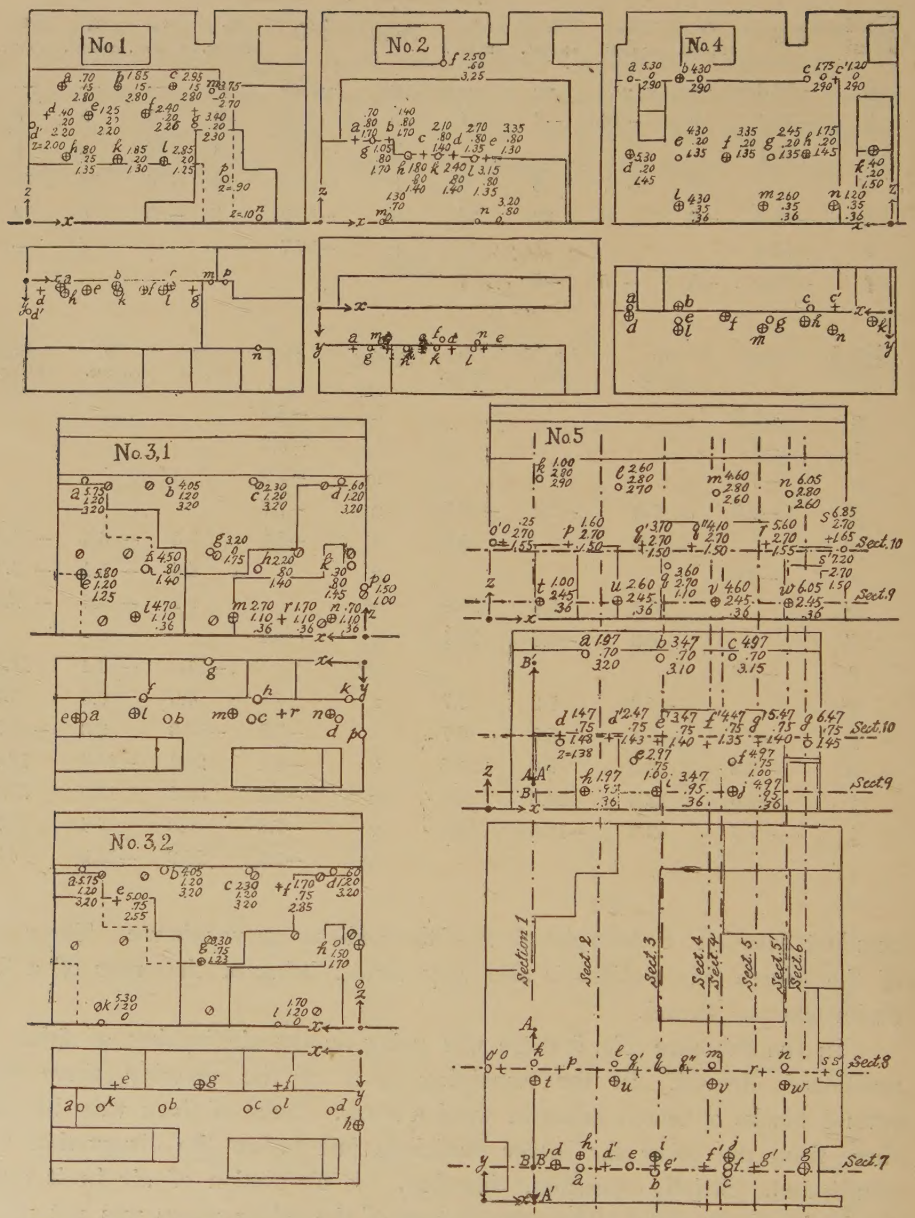

Fig. 4. The positions of points, at which, ○: the temperatures, and +: the velocities of circulation were measured. Annexd columns of figures give, each from top to bottom, x-, y-, and z-coordinates of each point. ⊘ in Part No. 3 are the points, where the temperatures measured in the models. Chain lines in Part No. 5 show the sections, of which the motion of air was photographed in the model. AA′ and BB′ show the parts, on section 1, where the velocities were measured in the model. Similar denotations on the other sections are omitted. Black dots at the corners indicate the origins of the coordinates, arrows showing the positive directions of each coordinates.

produced by the supply of heat from the freezing fish on one side and the absorption of heat due to the melting of colder frozen fishes on the other. The nature of circulations observed in the two series at different times, about a night apart, did not show any fundamental difference between them, although no observation was made at one and the same place in both series. From this point and also from the fact that the mass of fishes in air-freezing was very large, it can be assumed that the air-freezing was in progress slowly enough to keep the circulation of air in nearly steady state. The assumption will be justified below from the results of the experiments with the model too.

Preparation of models.

An ice-box, having the capacity of 103 cm. × 75 cm. × 54 cm., whose front doors and the side walls were replaced with glass plates, was employed to protect the models from the external influences on both the movement of air and the local temperature distribution in the latter. The models of the parts of the warehouse indicated in Fig. 3 were made one by one in the ice-box, with the ground of a brass plate, with walls in glass plates, or pasteboard sheets, and with wares in pasteboard or zinc sheets. The linear dimension of the models were 1/7 for the parts Nos. 1, 2 and 4; 1/6.8 for the part No. 3; and 1/25 for the part No. 5, of the original scales. The models were not perfectly similar to the original space especially in respect of the boundary walls, where there were no such separations in the original. In few cases, however, the difference in this point seems to affect much the results of experiments.

In the chamber No. 5, the fishes in freezing were, in the original case, put in wooden cages piled up in a block in lattice-like manner. In the model a set of 5 stripes of narrow glass plates, arranged in a vertical plane with the longer sides put horizontally and apart one from another by about the same distance as the breadth of each plate, was put in the position of the front surface of the block, and a heater of coiled nichrom wire of about 1.8 ohms was prepared in the interior of the glass stripes.

To adjust the temperatures on the boundaries, several other heaters of the same kind, as well as the coolers of lead pipes with water circulating in them, were arranged around the models or in the pasteboard blocks of wares. The models of blocks of the melting frozen fishes in the chamber No. 5 and the models of cooling pipes of brine refrigerator were made of zinc boxes

and running water was passed through them. When it was necessary, the water was cooled with ice or a refrigerator beforehand.

Observation of circulations in models.

In the models Nos. 1, 2, 3 and 4, in which the space was passage-like shaped, the circulation of air in a longitudinal vertical plane was exclusively observed. To visualize the motion of the air, smoke from a reservoir were led through several fine glass tubes opening in the model at suitable points. The smoke was sent as slowly as possible, by pressing gently a bellows attached to the reservoir. The direction of motion, in the longitudinal vertical plane, of patches of smoke was sketched, while the velocity of them was measured with a stop-watch in the neighbourhood of the points where the current-meter was set in the original case. The temperatures at the points, where the measurement of the temperature was made in the original case, were determined by thermocouples, whose junctions were fixed at the several points. In the case of model No. 3, where the position of the fixed junctions did not coincide with those points, the temperatures at those points were determined by the graphical interpolation.

In the model No. 5, the three-dimensional circulation was observed. The motion of the air was visualized at first by the smoke of senkô, but in the later experiments the smoke was replaced with the fine powder of aluminium. No device was necessary to send the smoke into the model other than a small reservoir directly attached to an upper corner of the model, of which the linear dimension was made far smaller than the other models. The disturbances imposed on the mode of general circulation were not appreciable, while the new patches of smoke were leaking from the reservoir into the model. The smoke had, however, to be supplied continuously, because of the rapid diffusion of it in the turbulent motion of air in the model. The aluminium powder was scattered instantaneously from the end of a fine glass tube inserted in the model through a corner. The coarser particles settled down almost at once, while the finer ones were floating in sufficient number for several minutes, the disturbances, arose with the shooting of the powder, having subsided in a few seconds. The light from an electric arc, collected in a plane through a cylindrical lens and through a slit, was cast to the model to illuminate laterally in succession the smoke or the aluminium powder in several longitudinal, transversal and horizontal sections of the model, and their motion was photographed with several seconds' exposure

from the direction perpendicular to the beams. As the smoke usually formed long filamental trains of patches in the turbulent circulations, the stripes on the developed plate, in some parts, especially where the speed of motion was slow, did not show the direction of motion of individual patches. In such a case, the motion of some images of the patches of smoke cast on the finder-glass of the camera was traced on a tracing paper labelled on the finder-glass, and they were consulted to discern the true direction of motion from the photographs. So far as the general motion of the air is concerned, the fact, that the fine particles of the smoke have possibly the relative velocities in the flow of air, as pointed out by Prof. T. TERADA and M. TAMANO[1], does not come into question, although the temporary formation of the irregular stripes of smoke just mentioned can have, of course, certain mechanism, relating to such a fact, in common with those fine stable smoke patterns observed by those workers with the periodic columnar vortices of air produced by convection. The aluminium powder printed the images on the plate sweeping long or short distances, according as the flakes fluttered for a long or short time in certain orientation against the beam[2] or they entered or left the irradiated space. Owing to the turbulence, the sweeping of each image was in various directions even at one and the same point. But the general motion was recognizable better than from the photographs of the smoke. It was rather convenient for the statistical study of the possible directions of turbulent motion, that the images of the particles did not sweep long continuous traces. As we could not obtain the speed of general motion from the photographs, the time needed for the patches of smoke or powder to travel definite distances was measured at leisure in each transversal section at the parts shown with AA′ and BB′ in Fig. 4. The temperatures were measured with a thermocouple, of which a junction was held at the end of a glass tube. The glass tube was held by hand so as to bring the end successively to the points, where the temperature was observed in the original case.

Each observation was commenced a few hours after the adjustment of heating electric current and of the temperature and the flow of cooling water was finished, that is, when the steady state was reached.

---

(1) TERADA, T. and TAMANO, M.: Further researches on periodic columnar vortices produced by convection. Tôkyô TD Kôkû Hôkoku No. 53, 4 (12), 1929, 447–470. See p. 465.

(2) For the special orientation of the flakes of the aluminium powder giving the strongest illumination see TERADA, T. and HATTORI, K.: Some experiments on motion of fluids. Tôkyô TD Kôkû Hôkoku No. 16, 2 (2), 1926, 96.

Table III

No. 1 Point	(Exper. 1) θ'°C	t'	(Exper. 2) θ'	t'	(Exper. 3) θ'	t'	(Exper. 4) θ'	t'	(Exper. 5) θ'	t'	t
f	26.4	0.06	27.3	−0.01	31.2	−0.04	29.8	−0.03	37.3	−0.42	−0.45
b	26.5	0.19	27.6	0.31	31.4	0.24	30.1	0.27	38.9	0.54	0.00
l	26.4	0.03	27.4	0.05	31.5	0.32	29.9	0.15	37.6	−0.24	0.22
c	26.2	−0.33	27.0	−0.34	30.8	−0.48	29.2	−0.45	38.2	0.12	0.22
θ_2' :	26.39		27.31		31.19		29.72		38.00	θ_2 :	−13.70
e	26.6	0.03	27.7	0.05	31.5	0.32	30.4	0.15	38.5	0.24	0.66
k	27.4	1.57	28.2	1.15	32.3	1.37	31.3	1.35	39.7	0.42	0.89
h	27.1	1.17	28.3	1.26	32.4	1.50	31.5	1.40	40.6	1.57	1.10
a	26.9	0.78	28.0	0.83	31.8	0.74	30.7	0.79	39.8	1.10	1.33
θ_1' :	27.03		28.11		32.02		30.97		39.65	θ_1 :	−13.25

No. 2 Point	θ'	t'	t	Point	θ'	t'	t
g	28.5	−0.74	−0.26	f	29.4	−0.13	0.77
m	29.9	0.16	−0.26	n	31.4	1.11	0.77
h	29.8	0.10	0.26	k	32.8	2.03	1.28
l	29.9	0.15	0.26	θ_1' :	31.2	θ_1 :	−11.91
θ_2' :	29.7	θ_2 :	−12.30				

No. 3, 1 Point	(Exper. 1) θ'	t'	(Exper. 2) θ'	t'	(Exper. 3) θ'	t'	(Exper. 4) θ'	t'	t
a	24.6	−0 10	24.4	−0.33	29.8	−0.50	24.8	−0.50	0.00
b	24.8	0.10	25.2	0.33	31.1	0.43	26.4	0.39	0.00
c	24.7	0.00	24.9	0.08	30.6	0.07	25.7	0.00	0.00
d	24.7	0.00	24.8	0.00	30.5	0.00	25.8	0.05	0.00
θ_2' :	24.7		24.8		30.5		25.7	θ_2 :	−13.6
e	25.4	0.70	25.6	0.66	31.3	0.57	26.6	0.50	1.33
f	25.2	0.50	25.5	0.58	32.0	1.07	27.0	0.72	0.17
g	24.7	0.00	25.1	0.25	31.7	0.86	26.4	0.39	0.17
h	25.1	0.40	25.3	0.42	31.0	0.36	26.4	0.39	0.33
k	24.8	0.10	25.0	0.17	30.5	0.00	26.1	0.22	0.00
l	27.1	2.40	27.5	2.25	34.2	2.65	29.2	1.95	1.83
m	25.2	0.50	25.5	0.58	31.4	0.64	26.8	0.61	0.66
n	24.8	0.10	25.0	0.17	30.1	−0.29	26.4	0.39	0.50
θ_1' :	25.7		26.0		31.9		27.5	θ_1 :	−13.0

No. 3,2 Point	(Exper. 1) θ'	t'	(Exper. 2) θ'	t'	(Exper. 3) θ'	t'	(Exper. 4) θ'	t'	(Exper. 5) θ'	t'	t
a	25.3	0.02	28.8	0.08	30.9	0.10	28.9	−0.02	26.6	−0.06	−0.20
b	24.3	−0.36	27.4	−0.43	29.2	−0.41	27.6	−0.42	26.6	−0.06	−1.40
c	25.5	0.10	28.9	0.12	31.1	0.17	29.9	0.30	26.9	0.01	0.60
d	25.8	0.21	29.2	0.23	31.2	0.20	29.4	0.14	27.3	0.12	0.80
θ_2' :	25.3		28.6		30.6		29.0		26.9	θ_2 :	−13.6
h	25.7	0.17	29.8	0.45	32.0	0.46	29.2	0.08	28.0	0.30	1.20
k	27.4	0.82	30.9	0.86	33.5	0.98	31.9	0.92	30.4	0.91	0.60
l	28.4	1.20	31.7	1.15	33.6	1.02	32.4	1.08	31.1	1.09	1.40
θ_1' :	27.9		31.3		33.6		32.2		30.8	θ_1 :	−13.1

No. 4 Point	(Exper. 1) θ'	t'	t	Point	(Exper. 2) θ'	t'	t
d	27.3	−0.69	−3.46	d	27.6	−0.67	−3.72
m	27.6	−0.22	0.86	n	28.0	−0.13	0.05
n	27.7	0.05	0.33	k	28.2	0.08	−0.49
b	27.9	0.25	0.33	e	28.3	0.27	0.32
l	27.9	0.30	0.60	m	28.3	0.28	0.60
a	28.0	0.52	1.40	b	27.9	0.31	0.05
θ_2' :	27.71	θ_1 :	−14.12	θ_2' :	28.09	θ_2' :	−14.02
k	28.1	0.53	− 0.22	g	28.4	0.49	0.87
f	28.1	0.56	− 0.49	a	28.6	0.68	1.14
g	28.4	1.08	1.14	l	28.7	0.82	0.32
h	28.5	1.17	2.22	h	28.8	0.94	1.94
e	28.6	1.32	0.60	f	29.0	1.15	−0.76
c	28.6	1.34	2.75	c	29.1	1.32	2.49
θ_1' :	28.35	θ_1 :	−13.75	θ_1' :	28.87	θ_1' :	−13.65

No. 5 Point	(Exper. 1) θ'	t'	(Exper. 2) θ'	t'	(Exper. 3) θ'	t'	(Exper. 4) θ'	t'
i	18.6	1.13	17.9	1.58	23.9	1.05	20.6	−2.37
q	17.1	−0.19	16.4	0.22	23.2	0.32	22.3	0.65
k	16.8	−0.38	15.4	−0.63	22.9	−0.03	21.2	−1.30
l	16.9	−0.29	15.8	−0.30	23.3	0.46	21.7	−0.48
t	16.8	−0.37	16.1	−0.04	22.2	−0.75	22.0	0.13
u	17.2	−0.02	16.0	−0.15	21.9	−1.10	21.8	−0.22
o	16.7	−0.48	14.9	−1.07	22.6	−0.35	22.8	0.96
e	18.1	0.70	17.7	1.38	23.5	0.67	22.3	1.52

No. 5 Point	(Exper. 1) θ'	t'	(Exper. 2) θ'	t'	(Exper. 3) θ'	t'	(Exper. 4) θ'	t'
m	17.2	−0.02	16.0	−0.09	23.4	0.54	22.2	0.30
s	17.1	−0.12	16.1	0.24	23.3	0.38	22.1	0.22
v	17.4	0.12	15.5	−0.52	22.4	−0.62	22.2	0.26
w	17.3	0.02	15.7	−0.41	22.6	−0.04	22.1	0.22
θ_2' :	17.28		16.14		22.92		21.93	
h	17.2	−0.04	18.1	1.72	23.7	0.81	23.7	3.05
n	17.3	0.02	16.2	0.02	23.5	0.65	22.2	0.39
j	18.0	0.65	18.3	1.92	24.5	1.72	22.8	1.52
b	20.0	2.33	16.8	0.56	23.5	0.59	22.0	0.05
g	18.7	1.23	17.6	1.33	25.0	2.26	22.6	1.09
f	19.0	1.48	16.7	0.46	24.4	1.61	22.7	1.40
d	18.2	0.75	17.6	1.33	23.1	0.24	22.8	1.52
a	17.5	0.23	16.5	0.35	23.4	0.51	22.3	0.65
c	20.4	2.70	17.6	1.33	23.4	0.54	21.6	−0.65
θ_1' :	18.46		17.26		23.84		22 50	

Point	(Exper. 5) θ'	t'	(Exper. 6) θ'	t'	(Exper. 7) θ'	t'	t
i	21.4	0.82	22.8	1.30	17.1	1.80	−0.71
q	21.1	0.18	22.1	−0.20	16.6	−0.32	−0.53
k	21.0	0.05	21.6	−1.20	16.7	0.10	−0.35
l	21.3	0.52	21.8	−0.80	16.8	0.43	−0.35
t	20.6	−0.68	22.3	0.30	16.6	−0.32	0.02
u	20.5	−0.96	22.2	0.05	16.5	−0.75	0.02
o	20.7	−0.59	21.0	−2.45	16.6	−0.32	0.20
e	21.4	0.77	22.8	1.30	16.8	0.53	0.20
m	21.3	0.55	22.0	−0.45	16.8	0.64	0.38
s	21.1	0.14	22.6	0.80	16.9	0.75	0.38
v	20.9	−0.14	22.6	0.80	16.5	−0.85	0.38
w	20.7	−0.55	22.6	0.80	16.6	−0.32	0.38
θ_2' :	21.00		22.19		16.71	θ_2 :	−8.11
h	21.6	1.04	22.9	1.50	16.5	−0.85	0.56
n	21.1	0.27	22.1	−0.15	16.8	0.32	0.75
j	21.5	0.91	22.0	−0.45	16.8	0.64	0.75
b	21.6	1.18	22.8	1.35	17.1	1.70	0.75
g	21.9	1.68	23.2	2.15	17.2	2.24	0.93
f	21.7	1.23	23.0	1.65	17.0	1.17	0.93
d	21.4	0.73	22.8	1.30	16.9	0.75	1.10
a	21.3	0.59	23.3	0.03	17.1	1.81	1.65
c	21.7	1.36	22.8	1.35	17.0	1.28	1.65
θ_1' :	21.53		22.67		16.94	θ_1 :	−7.56

Comparison of the temperatures.

The results of the measurement of temperatures are given in Table III. To compare the local distribution of temperatures, the points at which the temperatures were observed were classified into two groups, first of higher

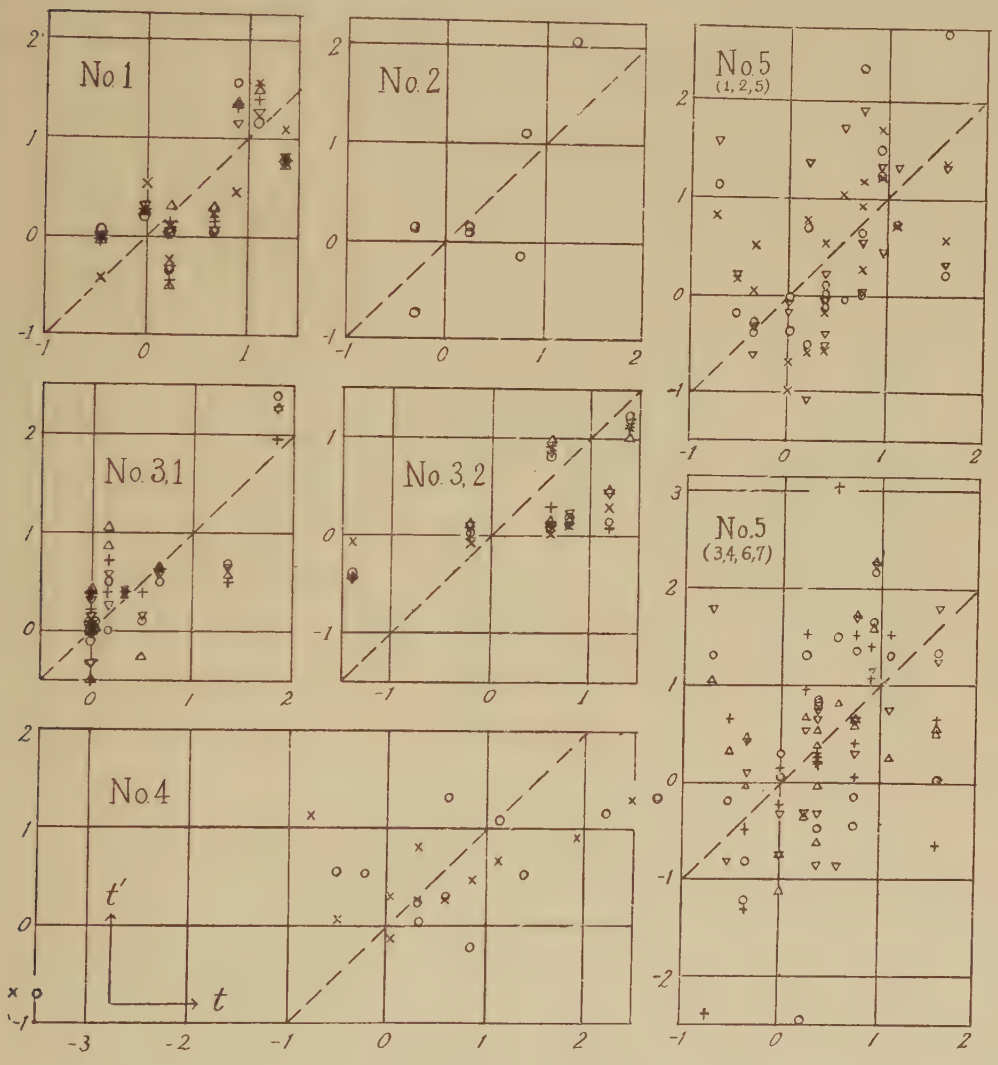

Fig. 5 Relation of the relative temperatures in models, t', to those in the originals, t.

Fig. 6 The directions of motion. Double arrows: determined from the records of the current meters; single arrows: from the sketches or photographs obtained with models; those with short separated segments, in No. 4, indicate the flow in the front part of the model.

and second of lower temperature, according as the temperature in the original case. For the part No. 3, the classification was made according as the position, upper and lower, and for the part No. 4, it was made according as the temperatures in the model of each point. The mean temperatures of both first and second groups were calculated both for the originals, θ_1 and θ_2, and for models, θ_1' and θ_2'. From the temperatures at several points, in the originals, θ, and in models, θ', the relative temperatures, $t=\frac{\theta-\theta_2}{\theta_1-\theta_2}$ and $t'=\frac{\theta'-\theta_2'}{\theta_1'-\theta_2'}$, were calculated and compared. They are also given in Table III. Fig. 5 shows the relation of t' to t. Although complete coincidence between t and t' is unexpectable, yet general similarity between the distribution of temperature in models and that of originals can be seen.

Comparison of the direction of motion.

By combining the components of velocities, obtained in the original case, the direction and speed of the general circulation in each section, in which the motion of air was observed in models, were determined. In the case of the chamber No. 5, where the points at which the current was observed in the original, did not lie on the planes of sections photographed, the components of velocity were first interpolated graphically and then the resultant velocity along the plane was composed. The direction of motion, thus obtained, is indicated by double arrows in Fig. 6, in which the direction of the general flow obtained from the sketches or from the photographs are described with fine arrows. Generally speaking, the modes of motions in the original and the modelled circulations are similar to each other, and especially so when the relative temperatures coincide closely.

Comparison of the speed of circulation.

Under the assumption of validity of the relation $V\propto(L.\Delta\theta)^{\frac{1}{2}}$ obtained in the preliminary study, among the speed, V, the linear dimension, L, of the general circulation and the local temperature difference, $\Delta\theta$, the comparison of speed of the original and the modelled circulations was made in the following manner:—

The differences of the mean temperatures, $\Delta\theta=\theta_1-\theta_2$ and $\Delta\theta'=\theta_1'-\theta_2'$, above mentioned, were employed as the representative local temperature differences, and from the speed at each point, V', measured in the models, the

Table IV

No. 1 L/L′=7.0, $\Delta\theta$=0.45 °C

Point	(Exper. 1) $\Delta\theta'$=0.64 V′	V″	(Exper. 2) 0.80 V′	V″	(Exper. 3) 0.83 V′	V″	(Exper. 4) 1.25 V′	V″	(Exper. 5) 1.65 V′	V″	V
	cm/sec.	cm/sec.	cm/sec.	cm/sec.	cm/sec.	cm/sec.	cm/sec.	cm/sec.	cm/sec.	cm/sec.	cm/sec.
b	5.3	11.7	5.9	11.7	6.5	12.6	7.3	11.5	6.9	9.4	10
d	6.2	13.7	9.8	19.4	9.1	17.6	9.6	15.2	9.3	12.6	28
e	5.2	11.5	4.3	8.5	6.6	12.8	6.4	10.1	7.3	9.9	13
g	6.0	13.3	8.1	16.0	8.7	16.9	6.8	10.8	12.0	16.3	10
h	6.0	13.3	11.1	22.0	9.6	18.6	9.1	14.4	9.3	12.6	11
k	7.2	15.9	11.4	22.6	9.3	18.0	9.3	14.3	13.6	18.5	11
l	6.3	13.9	8.2	16.1	8.2	14.9	7.0	11.1	12.9	17.6	13
Mean	6.0		8.4		8.3		7.9		10.2		13.7

No. 2 L/L′=7.0, $\Delta\theta$=0,39, $\Delta\theta'$=1.5

Point	V′	V″	V	Point	V′	V″	V
a	5.0	6.8	9	d	5.8	7.9	11
b	5.1	6.9	16	e	6.5	8.8	9

No. 3, 1 L/L′=6.8, $\Delta\theta$=0.6

Point	(Exper. 1) $\Delta\theta'$=1.0 V′	V″	(Exper. 2) 1.2 V′	V″	(Exper. 3) 1.4 V′	V″	(Exper. 4) 1.8 V′	V″	V
e	10.0	20.2	9.0	16.6	11.4	19.4	10.0	15.0	10
l	9.1	18.3	8.4	15.5	10.6	18.0	9.1	13.6	21
r	6.9	14.0	6.6	12.2	6.9	11.7	10.2	15.3	14
Mean	8.7		8.0		9.7		9.8		15

No. 3, 2 L/L′=6.8, $\Delta\theta$=0.5

Point	(Exper. 1) $\Delta\theta'$=2.6 V′	V″	(Exper. 2) 2.7 V′	V″	(Exper. 3) 3.0 V′	V″	(Exper. 4) 3.2 V′	V″	(Exper. 5) 3.9 V′	V″	V
e	7.0	8.0	9.1	10.2	8.2	9.6	7.7	7.9	6.2	6.8	9
g	6.1	7.0	6.9	7.7	6.9	8.1	8.0	8.2	6.1	6.7	10
h	10.0	11.4	9.8	11.0	8.9	10.4	7.5	7.7	9.8	10.8	10
Mean	7.7		8.6		8.0		7.7		7.4		9.7

No. 4 $L/L'=7.0$, $\Delta\theta=0.37$

Point	(Exper. 1) $\Delta\theta'=0.64$ V'	V''	(Exper. 2) 0.78 V'	V''	V	Point	(Exper. 1) V'	V''	(Exper. 2) V'	V''	V
b	7.7	15.5	6.7	12.2	11	h	6.7	13.5	6.7	12.2	6
c′	5.3	10.6	6.9	12.6	9	k	4.7	9.4	6.7	12.2	9
d	9.1	18.2	10.8	19.8	24	l	6.6	13.2	9.8	17.8	19
f	7.2	14 5	9.0	16.4	7	m	6.4	12.8	9.6	17.5	11

No. 5 $L/L'=25$, $\Delta\theta=0.55$

Sect.	(Exper. 1) $\Delta\theta'=1.18$ V'	V''	(Exper. 2) 1.12 V'	V''	(Exper. 3) 0.92 V'	V''	(Exper. 4) 0 48 V'	V''	(Exper. 5) 0.23 V'	V''	V
1AA′	6.7	23	5 0	18	4.0	16	3.6	19	3.5	27	28.0
BB′	5.3	18	5.6	20	2.2	8	—	—	5.0	38	—
2AA′	5.4	18	4 7	16	6 4	25	5.4	29	3.4	26	27.0
BB′	4.8	16	5.0	18	—	—	—	—	5.3	25	18.4
3AA′	3.8	13	4.9	17	7.8	30	3 4	18	3.4	26	21 6
BB′	5.3	18	5.9	21	—	—	—	—	3.3	25	25.0
4AA′	4 4	15	5.0	18	—	—	—	—	4.0	31	13.7
BB′	—	—	4 2	15	5.3	21	3.3	18	4.0	31	9.3
5AA′	6 7	23	4.4	15	—	—	3.4	18	4.7	36	23.7
BB′	1.3	4	—	—	7.7	30	3.9	21	—	—	7.4

Sect.	(Exper. 4) $\Delta\theta'=0.57$ V'	V''	(Exper. 5 0·53 V'	V''	V	Sect.	(Exper. 4) V'	V''	(Exper. 5) V'	V''	V
1AA′	4.0	20	3.6	18	23.0	4AA′	5.6	27	—	—	11.3
BB′	2.0	10	4.8	25	—	BB′	4.5	22	3.0	15	10.1
2AA′	7.0	34	7.0	36	27.0	5AA′	4.8	23	5.0	26	19.2
BB′	2.0	10	—	—	18.4	BB′	10.0	49	4 2	22	8.7
3AA′	6.4	31	6.7	34	21 6	6AA′	4.7	23	7 0	36	26.2
BB′	—	—	—	—	25.0	BB′	1.5	7	—	—	6 7

"estimated" speed, $V''\equiv V'\left(\frac{L}{L'}\frac{\Delta\theta}{\Delta\theta'}\right)^{\frac{1}{2}}$, was calculated and compared with the component of velocity on each sectional plane at each point. The results are given in Table IV and Fig. 7, from which we know that the "estimated" speed at each point coincides with the original one at least in the order of magnitude. It is rather remarkable that we get such a coincidence, notwith-

standing the roughness of observations in both temperature and velocity in the originals.

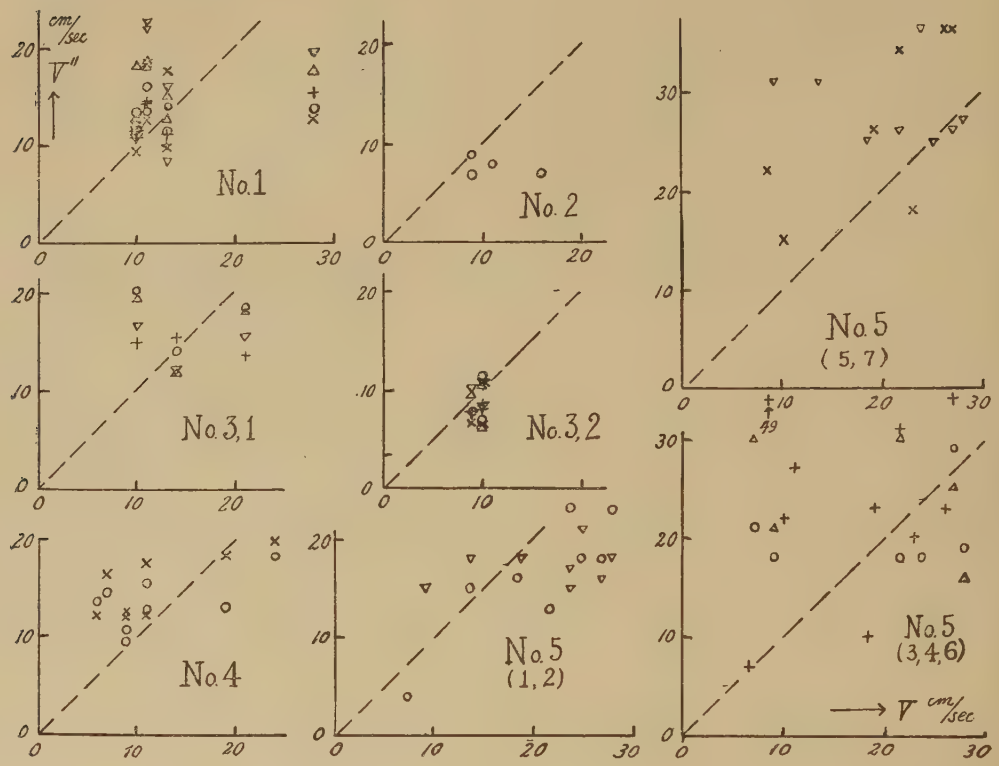

Fig. 7 Relation of the "estimated" velocities, $V''\equiv V'\left(\frac{L}{L'}\,\frac{\Delta\theta}{\Delta\theta'}\right)^{\frac{1}{2}}$, to the original ones, V.

Discussions of the results.

In order to verify the assumption, that the relation $V\propto(L.\theta\Delta)^{\frac{1}{2}}$ holds good, several series of experiments with some of the models were chosen.

In the experiments with the models No. 3, the local distribution of the temperatures, as well as the mode of circulation was made especially well similar to those in the originals. The speed at several points was averaged and with those averaged values, which are also given in Table IV, the relation between $\log V'$ ($\log \bar{V}$ for the originals) and $\log(L'.\Delta\theta')$ ($\log(L.\theta\Delta)$ for the originals) was examined.

Table V

No. 1. L=7.0, L′=1

$\log(L.'\Delta\theta')$	$\bar{1}.81$	$\bar{1}.91$	$\bar{1}.92$	0.10	0.22	$\log(L.\Delta\theta)$	0.50
$\log V'$	0.78	0.92	0.92	0.90	1.01	$\log \bar{V}$	1.14

No. 3, 1. L=6.8, L′=1

$\log(L.'\Delta\theta')$	0.00	0.08	0.15	0.26		$\log(L.\Delta\theta)$	0.61
$\log \bar{V}'$	0.94	0.90	0.99	0.99		$\log \bar{V}$	1.18

No. 3, 2. L=6.8, L′=1

$\log(L.'\Delta\theta')$	0.41	0.43	0.48	0.51	0.59	$\log(L.\Delta\theta)$	0.53
$\log \bar{V}'$	0.89	0.94	0.91	0.89	0.87	$\log \bar{V}$	0.99

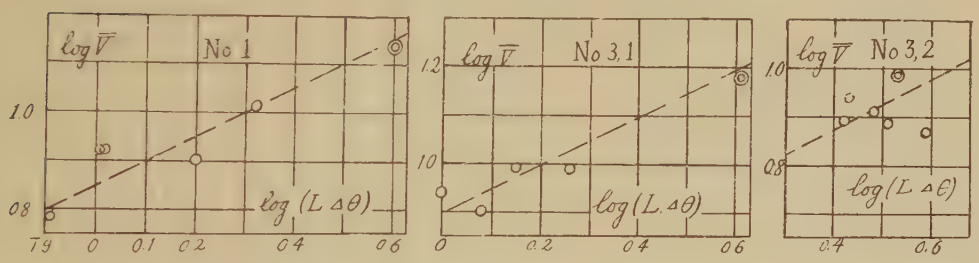

Fig. 8 Relation between $\log \bar{V}$ and $\log(L.\Delta\theta)$. ◎: for the originals; ○: for the models. Broken lines represent the equation, $\log \bar{V}=\frac{1}{2}\log(L.\Delta\theta)+C$.

As shown in Table V and Fig. 8, it is evident that the relation is expressed by the equations $\log V'=C+\frac{1}{2}\log(L'.\Delta\theta')$ and $\log \bar{V}=C+\frac{1}{2}\log(L.\Delta\theta)$, with one and the same constant C, i.e. with those averaged speed, the relation $V\propto(L.\Delta\theta)^{\frac{1}{2}}$ is valid.

In the experiments with the model No. 5, where the circulation was three dimensional, and the observation of the speed was made at many points, the degree of the dissimilarity between the local distribution of temperature in the original circulation and that in the models was represented by taking the standard deviation of the difference in the relative temperatures, $\Delta t=t'-t$, $\sigma_t\equiv\sqrt{\frac{\Sigma(\Delta t)^2}{n}}$, where n is the number of points. Similarly the degree of the false estimation of velocity was represented by the standard deviation,

Table VI

No. 5 Exper.	5	1	2	7	3	4	6
σ_t	0.22	0.75	0.77	0.82	0.88	1.02	1.45
σ_V cm/sec.	8.1	5.3	6.4	11.3	12.5	15.5	8.4

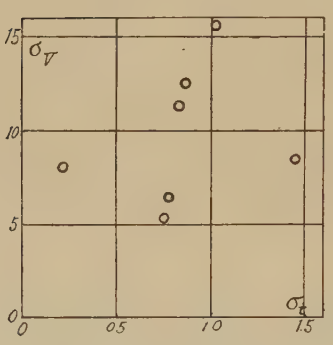

Fig. 9 Relation between the standard deviations of the differences of "estimated" velocities from the original ones to those of the differences of relative temperatures.

$\sigma_v \equiv \sqrt{\frac{\Sigma(\Delta v)^2}{n}}$, of the difference of the "estimated", V'', from the original speed, $\Delta V \equiv V'' - V$. The dissimilarity was thus considered to be due to some accidental causes such as the roughness of the observation or the difference in the surrounding conditions in the originals and in models. From the relation between σ_t and σ_v, as shown in Table VI and Fig. 9, it can be said that σ_v decreases as σ_t decreases and moreover that, when σ_t tends to zero, σ_v also tends to zero. In other words, the more similar the distribution of the temperature is, the closer the estimation of the speed becomes. This fact again supports the validity of the above relation.

Conclusions.

We can say that the laws obtained in the preliminary experiments are valid for the steady circulation of air in a cold-storage warehouse due to natural convection, and indeed not only when the general circulation is nearly two-dimensional, but also when it is three-dimensional. The circulation in the chamber, where the air freezing of fishes is going on, can also be treated as in quasi-stationary state.

The writer's cordial thanks are due to Prof. Morisaburô TAUTI for his kind guidance, and to Mr. Kiyohide MIYOSI, Mr. Hideaki YASUDA and Mr. Katumi YAMAGUTI for their laborious assistances in the observations and experiments, and also to Mr. Hideo WADA for helping the preparation to carry out the observation and to Mr. Ikurô HIROSE for the help in the improvement of the method of experiments. The writer expresses his best

thanks to Mr. I. MURAYAMA and Mr. S. KATO who have given him various opportunities in the Tobata Cold-Storage Company.

September 25, 1934. At the Physical Laboratory of
the Imperial Fisheries Institute.

Summary.

1. Distribution of temperature and the velocitiy of steady circulations of air produced by natural convection in several parts of a cold-storage warehouse were observed and were reproduced in a reduced scale in models.

2. It was proved that the laws of natural convections in the steady state, which were obtained in the preliminary study, are utilizable in the comparison between the original and the modelled circulations.

Explanation of Plates.

Pls. XXXII, XXXIII. Examples of photographs of circulations visualized with aluminium powder in the model of the chamber No. 5, at several transversal and longitudinal sections, which are indicated in Fig. 4 on page 236.

Sect. 1
Sect. 2
Sect. 3
Sect. 4

Sect. 7
Sect. 8
Sect. 5
Sect. 6

Experimental Studies of the Water Movement in Coastal Regions of the Sea. II. Tidal Oscillations in Sagami Bay. (II).

(Pls. XXXIV~XLV)

By Mituyo Okada and Kiyohide Miyosi.

(Received March 20, 1935)

For the purpose to examine to what extent and under what condition, the modelled water movements in coastal waters will reproduce various features of the originals, the previous experiments on the semidiurnal tidal oscillations in Sagami Bay, which are reported in the first paper[1], seem to fall a little short of our demand, chiefly because of too small number of points, where the tidal motion of the water surface was observed. It is very probable, on the other hand, that the incorrect direction, in which the tidal waves on the outside of the Bay were made to propagate, *i.e.* S 60°W instead of S 80°W, had decisive influence on the mode of propagation of waves in the interior of the Bay.

The experiment to be reported in the present paper, having been intended to meet better the aim of study, was carried out under an improved condition with respect to the wave generating arrangements. Special attention was turned to the movements on the outside of the Bay, besides in the interior. Detailed observations were performed in both the parts of the model. Although the results obtained are never fully satisfactory, they still show the mode of propagation of tidal waves in the region, and some of them will furnish us with the knowledge to be consulted in the further improvement of the experimental methods.

Improvements of the model and its attachments.

The ground of model basin was essentially unaltered. The scale of linear dimension was, as before, 1.25×10^{-5} for horizontal, and 1.75×10^{-4} for vertical

(1) Okada, M. and Miyosi, K.: Experimental Studies of the Water Movement in Coastal Regions of the Sea. I. Tidal Oscillations in Sagami Bay. J. Imper. Fisher. Inst., Vol. XXIX, No. 1, 1933, 15~98.

distances, respectively. The wooden barrier, *B*, which directed the movement of water across the ridge off Ôsima, was put in the new direction, N 79° E, passing about the midway from Miyake to Mikura Isles, as shown in Fig. 1. The teeth-formed guiding mouths of piston-canal, were accordingly entirely reconstructed.

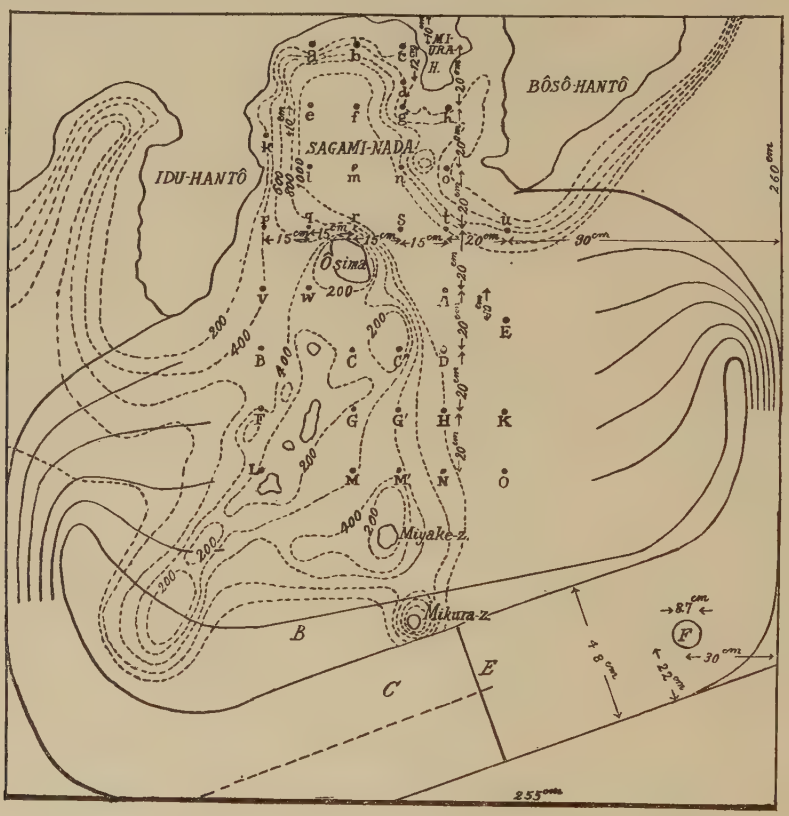

Fig. 1. Plan of the model, with attachments. Dotted lines: the isobaths in m. of original scale; a, b,.....w, A, B,.....N and O: the points at which the wave was observed; *B*: the barrier; *C*: the canal: *E*: the piston; and *F*: the vertical cylinder.

The fact being taken into account, that the range of tides was previously a little greater than expected, the breadth of canal of piston, *E*, and the diameter of vertically oscillating cylinder, *F*, were diminished, and the strokes of both piston and the cylinder were reduced to 17.5 cm. According to the provisional law of dynamical similarity, given in the previous paper, the period,

T, of oscillation was made about 42.3 sec. which correspond to the mean semidiurnal tidal period of 12.42 hours. The fluctuations in the period due to the variation of speed of driving motor, occasionally amounted to ± 1.5 sec. The steel wire, which suspended the vertical cylinder, was tied at the other end to the crank-disc of piston, subtending an average angle of 65° at the centre of disc with horizontal piston axis, so that the vertical cylinder sunk to its deepest position at the instant about $(65/360)\,T$ sec. before the piston assumed its eastern end-position. The angle was so determined that the high water should take place nearly at the same time as the maximum westerly current, as in the case of ideal progressive wave.

Methods of observation and measurements.

The methods of observation and measurements, employed in the previous experiments, were only slightly changed. Horizontal surface currents were recorded by taking photographs of the locii described by fine aluminium flakes scattered on the surface, during 3 seconds' exposure, commencing at every 12th division of the whole period, while the vertical oscillations of surface were optically recorded, by means of a special arrangement, as described in the previous report. The points, at which the wave was recorded were increased to 34 in number, and the surface currents were measured with micrometer microscope on the photographs at 37 points, including all of them (Fig. 1).

The range of tides was calculated by comparing the range of main wave with the maximum amplitude on the record and the maximum amplitude was converted to that of movements of surface, which were observed directly by aiming, with a microscope, at the top of shadow of a pin supported vertically above the surface. The length of optical lever of the tide registering arrangement from the vibrating mirror to the recording camera was in each case measured, and the tidal range on the record was again interpreted to that of vertical motion of the surface. The result of calibration of the arrangement has given the relation, that the vertical movement of 1 mm. of the water surface results a displacement of 3.0 cm.[1] on the record, when the optical lever is 100 cm. long, provided the optical beam reflecting at the mirror is nearly horizontal. In the experiment, the length of optical lever varied from about 180 to 280 cm., and the last condition was fulfilled almost always. The

(1) The vertical displacement of about 0.6 mm of the ring put on the surface of water results the same, the mechanical lever of the ring having an arm of 4.0 cm.

absolute values of range calculated by both methods generally stood in agreement with each other, as shown in Fig. 3.

No observation of the current beneath the surface was made.

Table I.

u: velocity in cm/sec.; α: direction measured *contra solem* from north.
The negative minimum current means the rotation *cum sole*
of the ellipse of tidal current.

Points	Maximum v	Maximum α	Minim. v	Residual v	Residual α	Points	Maximum v	Maximum α	Minim. v	Residual v	Residual α
a	.065	129°	+.015	.002	275°	v	.552	147°	+.088	.064	51°
b	.068	107°	+.007	.015	82°	w	.364	136°	−.099	.143	332°
c	.030	76°	+.003	.007	56°	A	.478	112°	−.006	.103	273°
d	.083	87°	+.013	.050	58°	B	.555	128°	+.166	.098	185°
e	.161	152°	−.000	.048	255°	C	.606	147°	−.004	.377	296°
f	.131	137°	−.007	.015	146°	C′	.389	101°	+.023	.376	294°
g	.138	108°	−.014	.052	4°	D	.456	108°	−.042	.268	281°
h	.088	108°	+.003	.063	151°	E	.382	113°	−.037	.154	262°
k	.150	174°	+.004	.006	45°	F	.782	108°	+.293	.360	216°
l	.308	140°	+.004	.188	280°	G	.404	78°	+.115	.457	50°
m	.245	120°	−.035	.152	249°	G′	.654	106°	+.023	.176	76°
n	.224	110°	−.008	.084	241°	H	.512	110°	−.029	.097	107°
o	.168	84°	+.063	.023	254°	K	.479	100°	−.033	.058	128°
p	.486	156°	−.011	.047	334°	L	1.06	108°	+.259	.206	66°
q	.520	149°	−.033	.037	135°	M	.698	120°	+.073	.359	320°
r	.496	96°	−.112	.113	237°	M′	.636	127°	+.146	.168	287°
s	.249	101°	−.045	.014	258°	N	.598	107°	−.035	.091	169°
t	.328	95°	−.035	.051	273°	O	.525	99°	−.020	.033	108°
u	.400	92°	−.023	.086	250°						

Results of observation.

Results of observation were also treated in the same way as those of the previous experiments, applying harmonic analyses to the mean curves obtained from the records of waves by free-hand smoothing of more or less vigorous disturbances, due to surface waves and secondary oscillations. North and east components of surface current were equally analysed. The phase and range of first harmonic waves, speed and direction of maximum, and mini-

mum velocities of the first harmonic tidal currents, as well as those of the residual current were determined. All kinds of phase were referred to the motion of the piston and the instant at which the piston came to its western end-position was chosen as 0° of it. The results are shown in Table I and in Figs. 2 to 4. Photographs of surface currents are all reproduced in the annexed plates. The number, i, put on the card in each photograph indicates that the latter was taken during each 3 seconds, commencing at the instant of the phase $30i$ degrees. Hence the values read on each photograph were attributed to the instant, whose phase is $30i + \{(3/2)/42.3\} \times 360$ degrees.

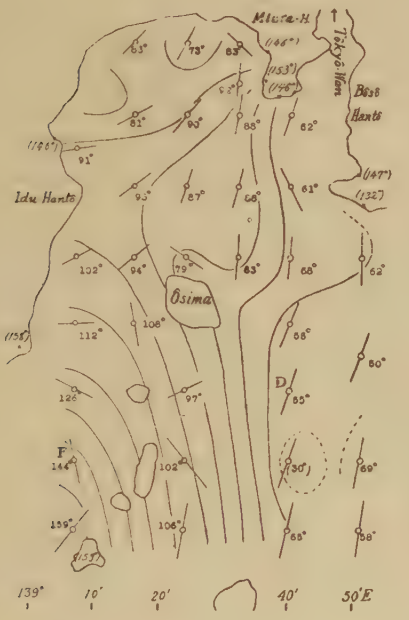

Fig. 2. Propagation of first harmonic wave. Full lines: the co-tidal lines inferred from the phase of high water, which is given by numerals at each point. Segments show the direction of the same, determined from elevation and current measurements. Bracketed numerals: the phase of M_2 tide given by Dr. S. OGURA.

Fig. 3. Range of vertical oscillation of water surface. Four numerals attached to each point are; in parenthesis: the maximum range including disturbances; the upper of the two below: range of the first harmonic calculated from the length of optical lever; the lower: calculated from the maximum range; and on the right side: their average.

Tidal Waves.

That the wave propagates from east to west on the outside of the Bay is evidently shown by the co-tidal lines, in Fig. 2, inferred from the distribution of phase of the wave. But, the speed of propagation is very small, as compared with the original M_2 tides. Thus, the difference in phase of M_2 tides at the south coasts of Bôsô and Izu Peninsulas is, according to Dr. S. Ogura's[1] report, about 26 degrees, while it amounts so great as about 82 degrees in the model.

Free long wave in an ideal fluid requires only 0.87 sec., which corresponds to 7.4° of difference in phase, to travel from the point D to the point F, the distance being 63.3 cm and the mean depth, 5.3 cm. As the discrepancy is very great, the wave generated in the present experiment is never of the nature of simple free long wave.

The irregularity in phase at such points as H and K, may partly due to the too short distances from the mouth of piston-canal.

The wave propagates in the Bay in somewhat complicated way, which entirely differs from that obtained in the previous experiments. It is of great interest, that the singularity in distribution of phase of M_2 tides along the coast of Miura Peninsula, *i. e.* a greater value, 153°, inserted between two smaller ones, 146°, as well as the equality in phase on both sides of the inner most part of the Bay, was almost completely reproduced in the model, although the absolute magnitude of the very difference in phase is evidently too great, as compared with original one. To the contrary, the equality of phase at the southern coast of Miura Peninsula on one side and the opposite coast on Bôsô Peninsula on the other, was not well reproduced. This is perhaps due to the effect of tides in Tôkyô Bay which was not constructed in the model.

The direction of co-tidal lines, obtained above, was checked by the law, expressing a similar idea as that of Proudman and Doodson[2].

In the case of waves in model in itself, the effect of earth's rotation is negligible, hence, if we also neglect tidal friction, the x- and y-components of horizontal velocity, u and v respectively, and the elevation of surface ζ, at time t, is connected by the equations of motion,

(1) Ogura, S.: The tides in the seas adjacent to Japan. Bull. Hydrogr. Dept. Imper. Japan. Navy, Vol. VII, 1933.

(2) Proudman, J. and Doodson, A. T.: Phil. Trans. Roy. Soc., [A] **224**, (1924), 185.

$$\frac{\partial u}{\partial t}=-g\frac{\partial \zeta}{\partial x}, \text{ and } \frac{\partial v}{\partial t}=-g\frac{\partial \zeta}{\partial y},$$

g being the acceleration due to gravity. Putting

$$u=u_1\cos\sigma t+u_2\sin\sigma t,$$

$$v=v_1\cos\sigma t+v_2\sin\sigma t,$$

and

$$\zeta=\zeta_1\cos\sigma t+\zeta_2\sin\sigma t,$$

where $\sigma=2\pi/T$, T being the period, we get

$$\left.\begin{aligned} \sigma u_2&=-g\frac{\partial \zeta_1}{\partial x}, \quad \sigma v_2=-g\frac{\partial \zeta_1}{\partial y},\\ \text{and}\quad -\sigma u_1&=-g\frac{\partial \zeta_2}{\partial x}, \quad -\sigma v_1=-g\frac{\partial \zeta_2}{\partial y}. \end{aligned}\right\} \quad \cdots\cdots (1)$$

From the expression $\zeta=H\cos(\sigma t-\gamma)$, on the other hand, we get

$$\zeta_1=H\cos\gamma, \quad \zeta_2=H\sin\gamma, \quad \cdots\cdots (2)$$

$$\left.\begin{aligned} \frac{\partial \zeta_1}{\partial x}&=\frac{\partial H}{\partial x}\cos\gamma-H\sin\gamma\frac{\partial \gamma}{\partial x},\\ \frac{\partial \zeta_1}{\partial y}&=\frac{\partial H}{\partial y}\cos\gamma-H\sin\gamma\frac{\partial \gamma}{\partial y},\\ \frac{\partial \zeta_2}{\partial x}&=\frac{\partial H}{\partial x}\sin\gamma+H\cos\gamma\frac{\partial \gamma}{\partial x},\\ \text{and}\quad \frac{\partial \zeta_2}{\partial y}&=\frac{\partial H}{\partial y}\sin\gamma+H\cos\gamma\frac{\partial \gamma}{\partial y}. \end{aligned}\right\} \quad \cdots\cdots (3)$$

Hence from (1), (2) and (3), we get

$$g\frac{H^2}{\sigma}\frac{\partial \gamma}{\partial x}=\zeta_1 u_1+\zeta_2 u_2,$$

and

$$g\frac{H^2}{\sigma}\frac{\partial \gamma}{\partial y}=\zeta_1 v_1+\zeta_2 v_2,$$

and for the slope, $\tan\varphi$, of the tangent line to the curve $\gamma=\text{const}$, we obtain the expression:

$$\tan\varphi=-\frac{\zeta_1 u_1+\zeta_2 u_2}{\zeta_1 v_1+\zeta_2 v_2}. \quad \cdots\cdots (4)$$

All factors in the right hand side of the equation (4) can be got from the

Table II.

$\zeta=\zeta_1\cos\sigma t+\zeta_2\sin\sigma t$: elevation of the surface; $u=u_1\cos\sigma t+u_2\sin\sigma t$ and $v=v_1\cos\sigma t+v_2\sin\sigma t$: east- and north- components of velocity.

Point	ζ_1 mm	ζ_2 mm	u_1 cm/sec	u_2 cm/sec	v_1 cm/sec	v_2 cm/sec	$\varphi=\tan^{-1}\left(-\frac{\zeta_1 u_1+\zeta_2 u_2}{\zeta_1 v_1+\zeta_2 v_2}\right)$
a	.007	.104	−.046	−.020	−.038	−.017	48°
b	.033	.109	−.065	−.019	−.018	−.011	63
c	.011	.091	−.029	−.003	+.008	−.003	−43
d	−.005	.124	−.079	−.024	+.004	−.002	85
e	.016	.102	−.068	−.035	−.126	−.065	29
f	.006	.108	−.081	−.041	−.088	−.035	50
g	.004	.102	−.110	−.069	−.045	−.010	81
h	.066	.123	−.079	−.037	−.025	−.015	71
k	−.002	.096	−.016	−.009	−.151	−.051	10
l	−.006	.104	−.179	−.080	−.213	−.102	38
m	.005	.103	−.167	−.134	−.121	−.040	72
n	.004	.120	−.191	−.088	−.073	−.024	75
o	.055	.100	−.148	−.078	−.016	−.063	−64
p	.015	.071	−.162	−.111	−.383	−.232	28
q	−.005	.100	−.236	−.136	−.414	−.163	41
r	.015	.080	−.425	−.249	−.102	+.070	−34
s	.014	.109	−.191	−.150	−.065	+.007	86
t	.048	.119	−.283	−.166	−.023	−.013	85
u	.059	.108	−.324	−.230	−.026	+.009	89
v	−.034	.081	−.287	−.112	−.349	−.298	− 2
w	−.033	.104	−.193	−.182	−.267	−.063	−80
A	.058	.085	−.382	−.223	−.159	−.086	68
B	−.051	.072	−.403	−.197	−.185	−.318	−27
C	−.011	.095	−.330	−.023	−.510	−.027	26
D	.033	.047	−.324	−.225	−.164	−.036	72
E	.059	.072	−.290	−.198	−.149	−.052	68
F	−.071	.038	−.680	−.081	−.122	−.382	−83
G	−.015	.073	−.385	−.096	−.043	−.128	−51
H	.035	.062	−.444	−.181	−.171	−.037	71
K	.036	.095	−.429	−.194	−.089	−.003	80
L	−.075	.026	−.778	−.595	−.395	+.035	53
M	−.027	.093	−.468	−.385	−.316	−.153	80
N	.030	.067	−.545	−.162	−.178	−.016	77
O	.060	.097	−.477	−.195	−.085	−.013	82

results of harmonic analyses. The direction of the co-tidal lines, thus determined for the present experiment is given in Table II. The segment attached to every circle indicating the point in Fig. 2 represents the tangent to the co-tidal line passing each point, which was determined in this way. The direction of such a segment coincides generally with that of co-tidal lines representing the distribution of phase, determined from ζ_1 and ζ_2 alone. Where they are not in coincidence with each other, the friction may not be neglected. At such points, either the depth is small or current is strong, or both are the case.

The fact that the wave reaches the coasts of Miura Peninsula and of Ôsima earlier than the deep between them, is in accordance with the findings of A. T. Doodson and R. H. Corkan[1] about the propagation of waves of M_2 tides in English Channel.

Tidal ranges found in model agree more closely in order of magnitude with those of original M_2 tides than those in the previous experiments. According to the law of comparison, 0.12 mm. correspond to 70 cm. of the range. The variation in its relative magnitude from place to place, however, is too great as compared with that of original M_2 tides, and moreover, the range in the model is greater toward northeast, while in the original rather toward southwest (Fig. 3). These discrepancies are essentially the same as in the previous experiments, and we have been unable to remove them by the improvement of model, such as described above. More fundamental improvement in the method seems to be necessary.

Tidal and residual currents.

Results of harmonic analyses of both components of velocity give the maximum current of the order ranging from 0.03 to 0.55 cm/sec. in the Bay, and from 0.4 to 1.0 cm/sec. on the outside of it. If the law of comparison given in the previous report holds good, 0.68 cm/sec. correspond to 1 knot, and, thus, the maximum current in the Bay is less than 1 knot, while on the outside, about 1 knot. These values do not seem to be too small, as compared with the speeds of semidiurnal tidal currents, given in Dr. S. Ogura's work[2].

Co-current lines are more complicated than co-tidal lines, as shown in Fig. 4. No such lines can be drawn to the south of Ôsima, where small whirls exist almost always. Such a whirl is of nature of stationary ones

(1) Doodson, A. T. and Corkan, R. H.: Phil. Trans. Roy. Soc., [A] **231**, 1934, 35.
(2) Ogura, S.: l. c.

rather than of those traveling with the general current. On the photographs of current, the change in position of each whirl can, as shown in Fig. 5, be traced from one plate to the next. Nothing has, however, yet been known of the existence of such whirls accompanying the original tidal currents.

Glancing at the photographs, we easily notice that there are in the Bay some belt-like narrow streams running accross or around the Bay, with greater velocity than the other parts. Some tracts of such streams are expressed with various lines with arrow-heads in Fig. 5. It is clearly shown by those lines, that there is more or less a discontinuity of the movement of water between two parts of the Bay, separated nearly by a line from Kawanazaki to Sunosaki. The discontinuity in the order of magnitude of the maximum current in these two parts can also be noticed in Fig. 4. According to Mr. K. KIMURA's private information, tidal currents influence but slightly the

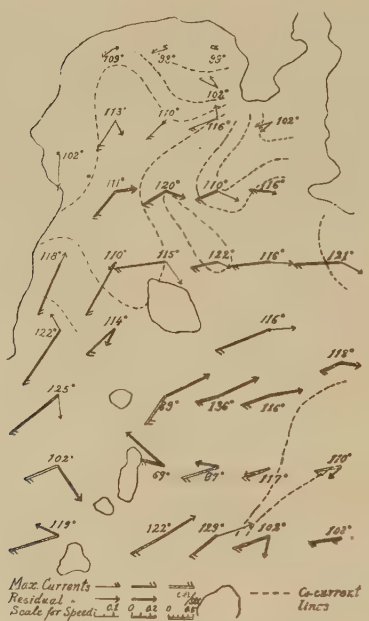

Fig. 4. Direction and speed of first harmonic maximum current and those of residual current. Attached numerals indicate the phase of maximum current, from which the co-current lines were drawn.

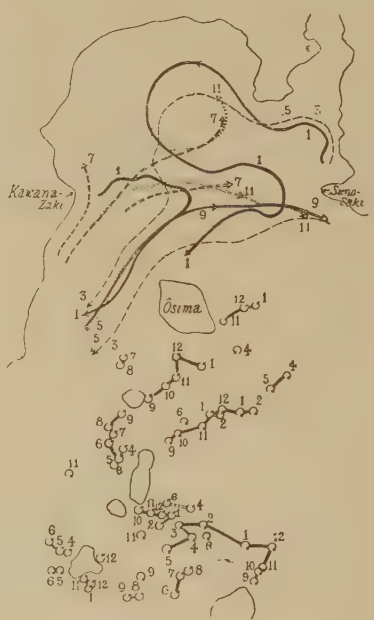

Fig. 5. Several tracts of belt-like streams of swift currents, and the movement of whirls near isles. Numerals refer to the number of photographs of surface current.

coastal current along the northern coast of the Bay, while considerably along the coast of Idu Peninsula, south of Kawanazaki. Strong tidal currents near Sunosaki described in the chart No. 80 of the Hydrographical Department of Imperial Japanese Navy, is not well reproduced in the experiment. It is perhaps due to the effect of tides in Tôkyô Bay.

In the strait between Idu Peninsula and Ôsima, current from north-east is strong near Ôsima, as in plates 1, 3 and 5, while that from south-west is strong near Idu Peninsula, as in plates 7 and 11. Consequently, there exists a clockwise circulation of the residual current as shown in Fig. 4. A greater circulation of the same sense is also observable off south-east of Ôsima, which may, however, be much influenced by the existence of the artificial boundaries to the east and south of it.

Conclusions and Summary.

The reproduced tides and tidal currents in the present experiment, have some features more or less in common with the original semi-diurnal tides. The great inconsistencies are seen in (1) the relative distribution of the range and (2) the absolute magnitude of difference in phase of tides at various points.

The order of absolute magnitudes of range and of speed of surface current is nearly in agreement with the provisional law, given in the previous report.

It is remarkable, that the irregularity in phase of M_2 tides along the coast of Miura Peninsula, and the difference in order of magnitude of tidal current between the northern and southwestern coasts of the Bay is evidently reproduced in the model.

To remove the discrepancies above stated, more fundamental improvement of the method of experiment seems to be necessary.

The witers' thanks are due to Prof. M. Tauti and to Mr. K. Kimura for the kind information.

March 15, 1935.

Physical Laboratory of the
Imperial Fisheries Institute.

PL. XXXV

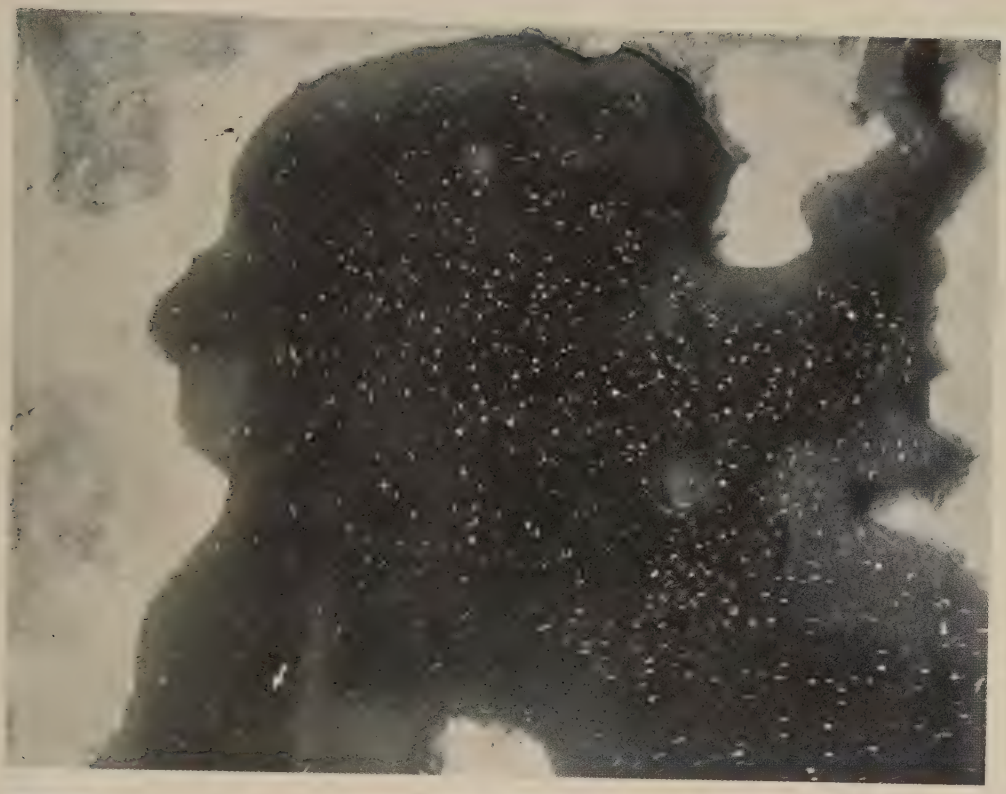

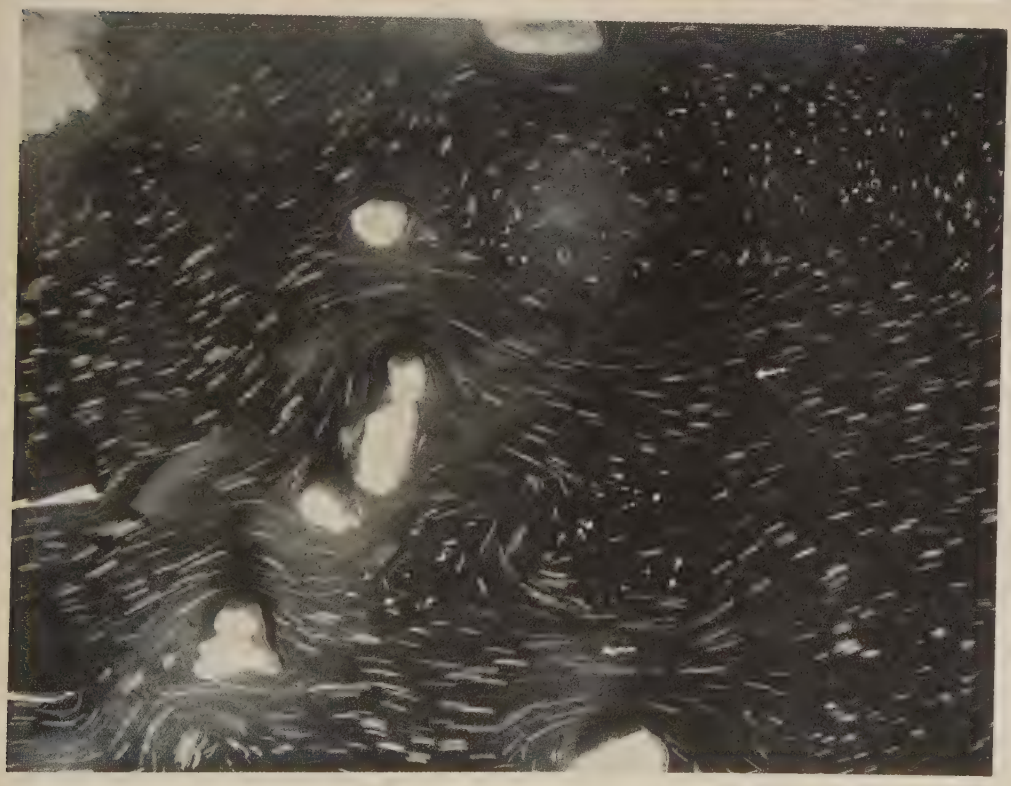

PL. XXXVII

PL. XXXIX

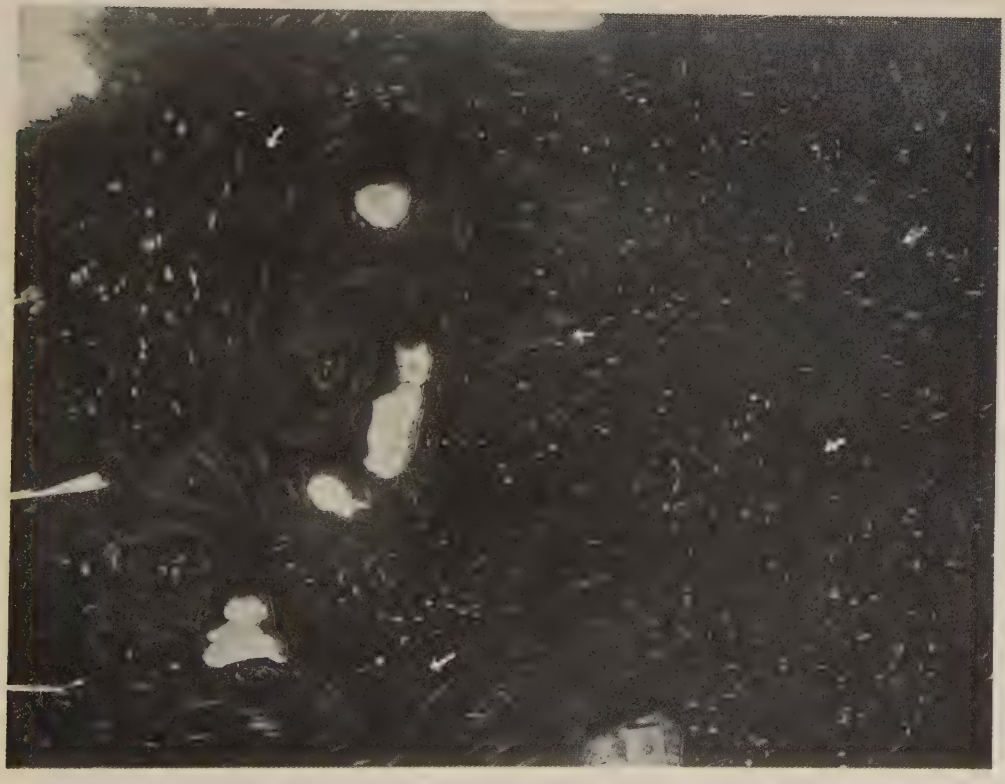

PL. XL

PL. XLI

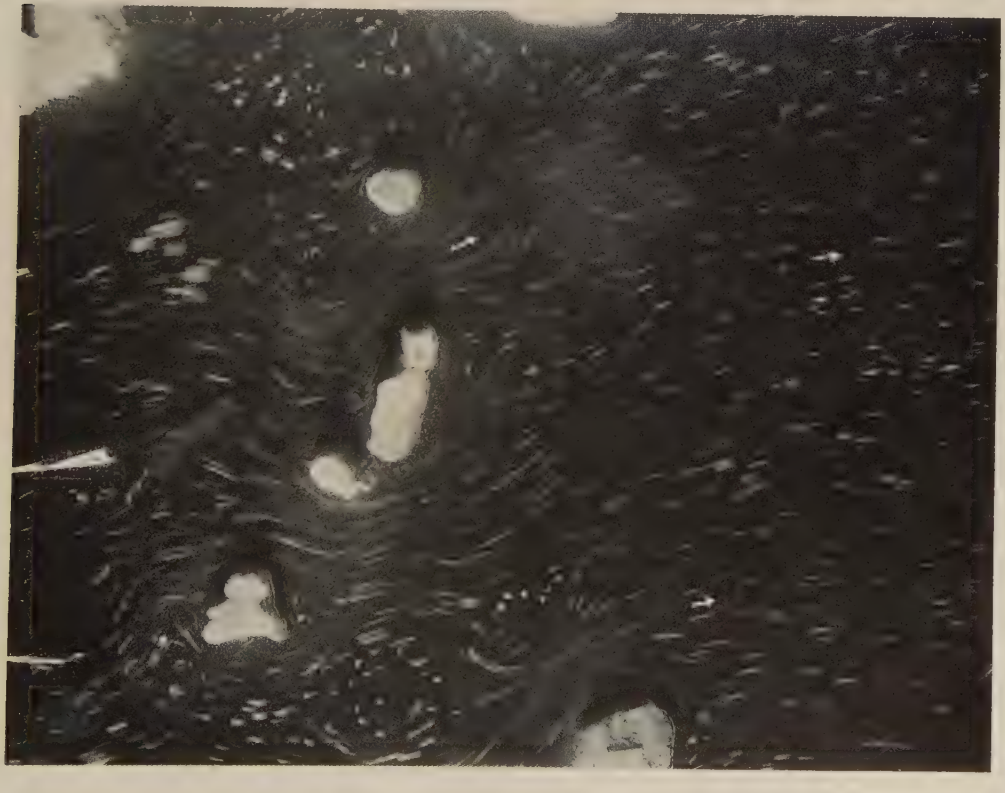

PL. XLII

PL. XLIII

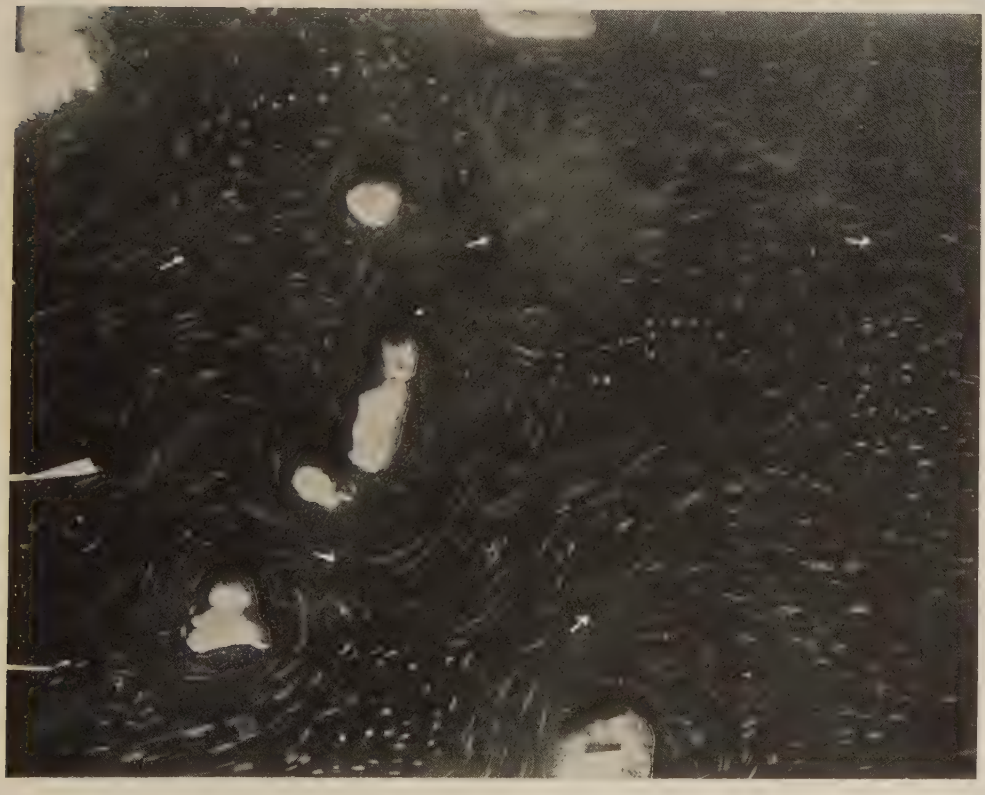

PL. XLIV

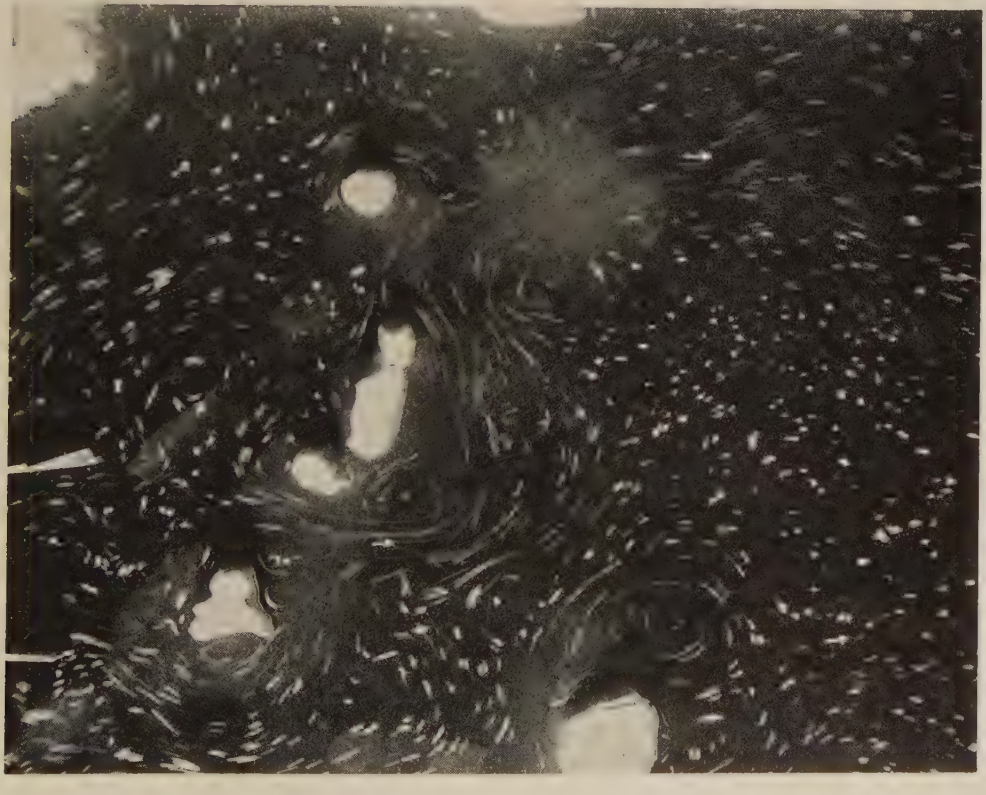

PL. XLV

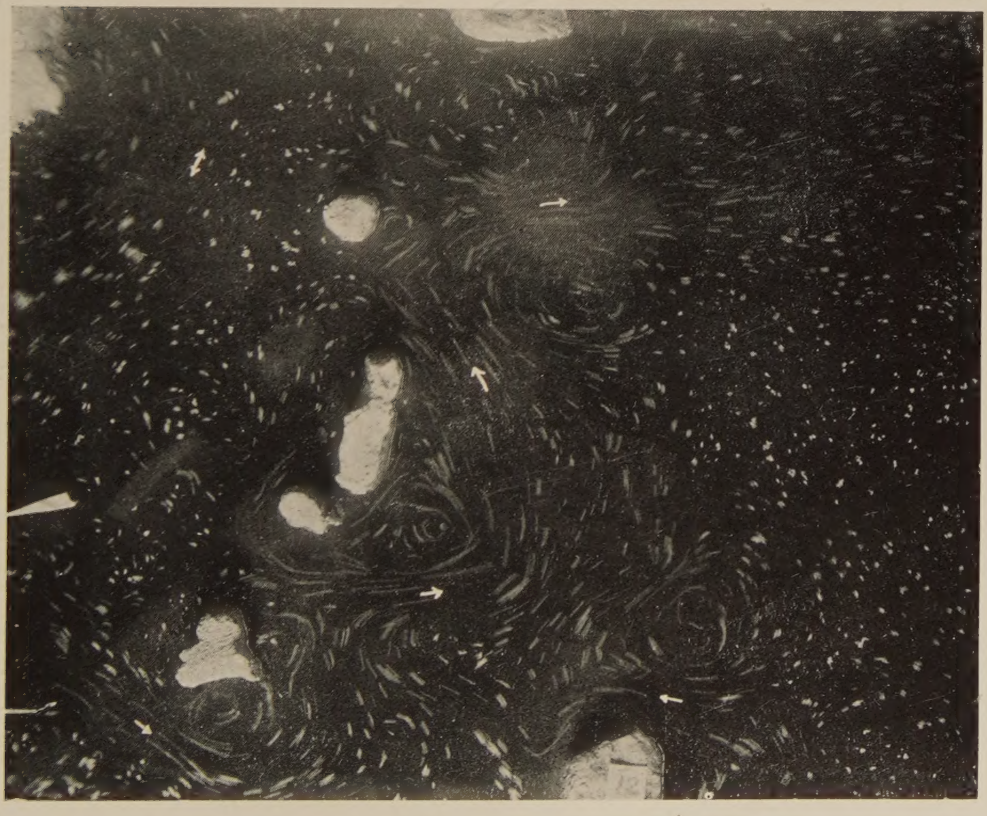

INDEX to Vol. XXX.

* Pages Illustrated

Page

Aka-demekin (Red telescope-eyed gold-fish) (Pl. VI) 11
All transparent-scaled character (Pl. IX) 60, 65
Anal fins [Gold-fish] (Pl. XII) 67
Apogon kominatoensis n. sp. 211, 212*
Arginine 98
Calico (Pl. VI) 19
Circulation of air [Cold-storage warehouse] (Pls. XXXII, XXXIII) 227
Chôtengan (Astoronomical telescope-eyed gold-fish) (Pl. VI) 13
Caudal fins [Gold-fish] (Pl. XI) 67
Clariger papillosus n. sp. 214, 214*
Comet (Iron-fish) 19
Concretions (Pls. XV, XVI) 117
Co-tidal lines 258
Current meter ..... 228~232, 228*
Demekin (Telescope-eyed gold-fish) 11
Desmid-flora (Pls. XVII~XXXI) 123
Fukinagashi (Streamer) 6
Genealogy [Gold-fish] 28, 30*
Gold-fish ..... 1~96
Hanafusa (Pl. VI) 16
Hibuna (Pl. VI) 5
Hozukius, gen. nov. 199, 200*, 202*, 203*, 204*
Iron-fish (Comet) 19
Jikin (Pls. I, VI) 13
Kinranshi (Pl. VI) 17
Kurodemekin (Black telescope-eyed gold-fish) (Pl. VI) 12, 38
Mendelian Inheritance [Gold-fish] (Pls. I ~XII) ..... 37~96
Monoaminoacids 104
Mosaic transparent-scaled character (Pl. IX) 65

Page

Nagasaki (Onaga) 6
Nankin (Pl. XI) 10
Narial Bouquet 16
Net-like transparent-scaled character (Pl. X) 65
Normal-scaled character (Pl. IX) 60, 65
Ocynectes maschalies Jordan & Starks 219, 220*, 222*, 224*
Okame 8
Onaga 6
Oranda-shishi-gashira (Pl. VI) 15
Osaka-Ranchû (Pl. VI) 10
Pebbles (Pl. PIV) 117
Principle of dynamical similarity of natural convection 227
Protamine 97
Pseudo-concretions (Pl. XIII) 117
Ranchû (Pl. VI) 8
Ranchû (Maruko) (Pl. VI) 8
Ryûkin (Pl. IV) 6
Sagami Bay (Tides and tidal currents in) 253
Salmine 97
Salmine sulphate 98
Sandstone 119
Sanshoku-demekin (Calico telescope-eyed gold-fish) (Pl. VI) 12, 38
Scorpaenoid fish 199
Sebastichthys (*Pteropodus*) *latus*, sp. nov. ... 208
Sebastichthys (*Pteropodus*) *longispinis*, sp. nov. 209
Sebastodes (*Primospina*) *wakiyai*, sp. nov. ... 205
Sebastodes (*Zalopyr*) *kawaradae*, sp. nov. ... 207
Sebastodes (*Zalopyr*) *melanostictus*, sp. nov. 206
Shishigashira (Lion-head) 8
Shubunkin (Pl. VI) 17
Shûkin (Pl. VI) 17

Telescope-eyed character 38
Tetsugyo (Iron-fish) 19
Tetsu-wonaga (Iron coloured long tail gold-fish) (Pl. VI) 15
Tidal Current [Sagami Bay] (Pls. XXXIV ~XLV) 257
Tidal range [Sagami Bay] 255
Tokin 8
Tosa-kin (Gold-fish of Tosa) 14
Variations [Gold-fish] 20
Varieties [Gold-fish] 2
Wakin (Pl. VI) 2
Watônai (Waryû) (Pl. VI) 16